Affinity-triggered hydrogels: developments and prospects in biomaterials science

Cláudia S. M. Fernandes, Ana Sofia Pina, Ana Cecília A. Roque*

Dr. C.S.M. Fernandes, Dr. A. S. Pina, Prof. A. C. A. Roque
UCIBIO, Chemistry Department, School of Science and Technology, NOVA University of Lisbon, Campus Caparica, 2829-516 Caparica, Portugal
E-mail: cecilia.roque@fct.unl.pt

Keywords: affinity interactions; physical hydrogels; self-assembly; protein biomaterials; multicomponent hydrogels

Molecular recognition events comprise the establishment of intricate networks of specific transient interactions between ligands and receptors. These occurrences are ubiquitous in Nature and key for Life as they regulate cells and organisms. As such, it is not surprising that the affinity and selectivity associated to molecular binding events have been the focus of research efforts, which further fed technological advances in diverse fields as medicine and materials science. One example includes the use of affinity interactions between building blocks comprising ligands and cognate receptors, as the driving force to trigger the self-assembly process of supramolecular architectures, thus creating materials with emergent properties. Over the last 20 years, different affinity pairs ligand-receptor, with a broad range of binding constants and displayed in a multivalent way using several approaches, have been explored to assemble physically cross-linked hydrogels with tunable properties. This review provides a summary and comparison of the strategies employed so far to design and generate affinity-triggered hydrogels, and presents the developments and challenges of these interdisciplinary biomaterials, which intrinsically combine protein engineering and material design, in the fields of tissue engineering and drug delivery.

1. Introduction

Life is maintained through a myriad of specific ligand-receptor interactions that trigger finely tuned reactions in cells and play a key role in metabolism. Examples of the importance of affinity interactions in regulating cells and organisms include protein-protein interactions controlling cellular signaling pathways, and antibody-pathogen recognition triggering the immunological defense in mammals.

Understanding how cells, tissues and organisms work in an orchestrated way is intrinsically related to the study of key biological players involved in natural molecular recognition events. Such knowledge then boosts several biomedical and technological advances based on the manipulation of the interactions between ligands and receptors. The universe of molecular architectures that can be explored to define new ligands with tunable affinity and selectivity towards a defined target is not restricted to natural ligands, and includes engineered peptide and protein architectures [1], or peptidomimetics and synthetic scaffolds [2,3]. An excellent example of engineering molecular recognition for different purposes is the exploitation of the interaction between bacterial protein A derived from *Staphylococcus aureus* and antibodies to develop affinity chromatography adsorbents, currently used in biopharmaceutical industrial settings to obtain pure antibody preparations [4,5]; and the engineering of the protein A fold to develop novel biomedical tools in imaging and therapy against non-cognate partners [6,7].

Within the materials science field, molecular recognition is typically used to add a particular function. For example, affinity and selectivity towards a defined biological target can be achieved through the immobilization of ligands onto 2D and 3D materials. These functional materials find applications in biosensing and biomaterials design. In the latter, a typical approach is to control the biological activity of materials by incorporation of adhesive peptides containing the sequence arginine-glycine-aspartic acid (RGD), which promote the attachment of numerous cell types [8–11].

An alternative way of interfacing molecular recognition with material science is to use affinity interactions (from 10^4 to 10^{15} M^{-1}), as the driving force to promote the self-assembly of multicomponent building blocks containing ligand and receptor molecules. Such a process may generate macroscopic materials, typically hydrogels, which represent an important class of physical hydrogels that combine the knowledge of material scientists and peptide/protein engineers. The selective molecular recognition, the broad range of binding constants of available affinity pairs and the existence of diverse multivalency systems, make affinity-triggered hydrogels a versatile and promising tool to generate complex, dynamic, synergistic, tunable and highly functional materials.

This review article focuses on affinity-triggered hydrogels promoted by the establishment of specific interactions between surfaces, typically found in protein-protein and protein-ligand (where ligand is a peptide, a sugar or a small ligand) interactions. As such, the manuscript will not address other affinity-based supramolecular hydrogels formed by host-guest interactions and molecular switches, which represent also a very rich literature source on designed and tunable biomaterials [12–17]. In the present paper, a brief introduction to hydrogels, and the differences between chemically cross-linked and physically cross-linked hydrogels is given first. In the second part of the review, the critical aspects to be considered in the design and application of affinity-triggered hydrogels are given, namely (1) an overview of affinity pairs ligand-receptor already explored, (2) a summary of the ways to generate multivalency, and details about the requisites of hydrogels for tissue engineering and drug delivery applications. The third section of the article provides an overview of the examples of affinity-triggered hydrogels reported over the last 20 years. Finally, the current challenges of affinity-triggered hydrogels and future directions in the field are discussed.

2. Chemically and Physically Cross-linked Hydrogels

Hydrogels are three-dimensional macroscopic networks comprising of insoluble networks of hydrophilic polymers, either natural or synthetic [18–20]. Hydrogels present solid-like mechanical properties and contain 90-99 % of water [21]. Despite the large amount of water absorbed, hydrogels maintain their structural integrity due to their chemical or physical networks [18]. The first description of a hydrogel reports back to 1960, when Wichterle and Lim [22] polymerized and cross-linked 2-hydroxyethyl methacrylate into a transparent gel for the manufacture of contact lenses. The goal was to develop a material that could substitute plastics in the field of alloplastic and prosthetics, but with a higher biocompatibility and permeability to metabolites. Since then, research on hydrogels moved towards various biomedical applications, including for example cell encapsulation [23] and/or implantation [24,25], wound healing [26], cartilage repair [27], cardiomyocytes mimics [28] and neurite growth [29]. Novel methodologies that dynamically tune hydrogels properties in a controlled fashion open several opportunities in the biomaterials field [30]. Hydrogels can be classified on the basis of several criteria [31], although the most conventional way is to perform the classification based on the preparation method, including the type of crosslinking mechanism used [32]. In this sense, hydrogels can be classified in chemically or physically cross-linked. The main characteristics of chemically and physically cross-linked hydrogels are summarised in Table 1 and Figure 1.

Chemically cross-linked hydrogels are assembled and maintained by strong covalent bonds (typically 40-100 kcal/mol) formed between polymeric chains through the aid of cross linkers. The establishment of covalent bonds between polymeric chains imply that compatible functional ends exist at the polymer backbone or side chains (naturally or added by chemical modification of the polymer chains), and that these groups can form covalent bonds upon activation by chemical agents (e.g. a suitable chemical cross-linking agent; a reaction catalyst; and enzymatic reaction) or physical stimulus (e.g. light). An extremely relevant class of chemical hydrogels are those assembled via click-chemistry reactions, in particular those based on biocompatible reactions [33]. In comparison

to conventional chemical routes, click-chemistry approaches increase the speed, yield and selectivity of the reactions, augmenting the control and precision over the gelation process [30]. The covalent bonds formed between hydrogel components, despite being strong in nature, can be irreversible or reversible on-demand thereby influencing the hydrogel properties, as recently reviewed [32].

Physical cross-linking between polymer chains or hydrogel components occurs without the need to perform further chemical modifications. In these cases, gelation depends on the intrinsic properties of the hydrogel components, and can be usually reversed upon modifying the environment, therefore offering dynamic systems [34]. When using natural polymers, gelation can be typically triggered by changes in temperature (e.g. physical entanglement in gelatin) or by establishing ionic interactions (e.g. alginate). Physically cross-linked materials can also be assembled on the basis of supramolecular chemistry. The process is fairly independent on the addition of organic solvents or chemical cross-linkers [35], but is influenced by environmental cues such as pH (when the solubility of the gelator is modulated around the pK_a of protonated groups in the molecule) [36], salt concentration (which reduces the effects of electrostatic repulsion between the components) [37] or solvent polarity (when the solubility of the gelator is higher in organic solvents than in water) [38]. The formation of the hydrogel network can also be triggered enzymatically, when an enzyme converts a soluble precursor into a supramolecular hydrogel [34,39]. Here, a myriad of weak non-specific and non-covalent bonds (e.g. electrostatic and ionic, hydrogen bonds, hydrophobic and π- π stacking, and van der Waals), individually with 0.1-5 kcal/mol, are established and concerted to form stable nanostructures, which further originate complex macroscopic assemblies. Amphiphilic peptides [40] and coiled-coil peptides, which self-assemble into a helical structure and a hydrophobic face [41], originate hydrogels maintained mainly by hydrophobic interactions. β-hairpin assembly peptides [42] and orthogonal self-assembly via molecular stacking of ureido-pyrimidinone motifs [43–45] explored hydrogen bonding to form hydrogel networks. The

electrostatic interactions between heterotrimeric helices of collagen-like peptides [46] have also been explored to form physically cross-linked hydrogels. Another example of physical hydrogels is those formed upon the establishment of non-covalent but specific interactions between hydrogel components, which can be considered as affinity-triggered hydrogels. Here, crosslinking greatly depends on the selectivity and binding affinity between the hydrogel components containing the two complementary moieties [47]. The great advantage of affinity-triggered hydrogels is that the assembly process relies only on the molecular interactions between the affinity pair, without requiring any external stimulus. Therefore the hydrogel network can be formed at physiological conditions, which is desirable for cell-related applications [9].

3. Affinity-triggered hydrogels

Affinity-triggered hydrogels are multicomponent systems. Typically, two components are used, each one containing a member of the affinity pair ligand-receptor. The ligand and the receptor establish specific non-covalent interactions between each other. The key parameters to be considered when assembling an affinity triggered hydrogel – affinity pair and multivalency - merge the knowledge from protein engineers and material scientists, and further impact the final application of the materials. Moreover, polymer weight, polymer concentrations, chain rigidity and crosslinking density can also be tuned to obtain hydrogels with the desired properties. This section will detail aspects related with the affinity pairs used for the generation of hydrogels, as well as the strategies available to generate multivalency, and finally discuss the main applications found for affinity-triggered hydrogels.

3.1. Ligand-receptor pairs for hydrogel formation

Nature is generous in the amount and diversity of affinity pairs ligand-receptor. However, not all reported affinity pairs can be easily manipulated outside the cellular environment, usually due to

their complexity, low stability or lack of information for production in host systems. As such, the real number of affinity pairs explored for the assembly of hydrogels is smaller than that offered by Nature, and can be grouped in systems that include peptide-peptide, protein-peptide, protein-small ligand, protein-protein or carbohydrate-peptide/protein (Table 2 and Figure 2). While most examples report natural biological ligand-receptor partners, there are a few systems where the ligands or receptors have been engineered to improve affinity, selectivity or stability (e.g. WW domain CC43 a computer derived WW domain with improved affinity towards the target peptide) [9]. The details of each affinity pair used so far to assemble affinity-triggered hydrogels are detailed in section 4.

The non-covalent interactions established between hydrogel components containing ligand and receptor occur through different binding events and are characterized thermodynamically by equilibrium constants (the affinity or association constant, K_a) and kinetically (by association, k_a, and dissociation rate constants, k_d). The equilibrium constant is directly related to the free energy levels of the bound and unbound complex. As the bound complex becomes more energetically favourable, the degree of association increases, until a contiguous network is formed. A more detailed overview of how physically-cross-linked hydrogels are governed by these constants has been reviewed elsewhere [48]. The determination of affinity constants (Ka) in an affinity pair ligand-receptor, can be performed by a wide variety of experimental methods, namely surface plasmon resonance, isothermal titration calorimetry, NMR spectroscopy, ELISA methods, microscale thermophoresis, atomic force microscopy, among others [49], or *in silico* using molecular modelling approaches [50].

3.2. Strategies to generate multivalency

In order to create affinity-triggered hydrogels each component of the affinity pair must be prepared in a multivalent manner to ensure the formation of a network (Figure 3). For example, Yamagushi

and Kiick [51] explored the affinity pair heparin/HIP peptide affinity pair (Ka = $2.5x10^5$ M^{-1}): they did not observe the formation of a gel when one of their hydrogel components was mixed without being displayed in a multivalent way; when both components were displayed in a multivalent way and were mixed, they observed the instantaneous formation of a hydrogel. To obtain the multivalent display of the components, three strategies have been used: (i) multimeric proteins can be used as one of the components (Figure 3A); (ii) the affinity pair components are displayed in tandem (Figure 3B); (iii) multimeric polymers are used as carriers where the affinity pair components are immobilized (Figure 3C-D). All these strategies can be combined between each other to form the network of an affinity-triggered hydrogel, as will be further discussed in the examples described in section 4.

3.2.1. Multimeric proteins

In Nature, several proteins are arranged as multimeric displays (Figure 3A), namely the tetrameric haemoglobin, the pentameric immunoglobulin M or the dimeric glutathione. When they are mixed with the corresponding receptor component, also displayed in a multivalent way, the hydrogel network forms as each component can simultaneously interact with more than one complementary molecule. Multimeric proteins can be directly purified from natural sources or produced in host organisms through recombinant DNA technology. Typically, the second option increases the production yields and the possibility to introduce mutations and protein modifications for improved selectivity or affinity towards the target receptor [52]. The design of a hydrogel using multimeric proteins is also limited by the intrinsic properties of the protein (e.g. solubility and hydrophobicity), which limits the physical and chemical properties of the resulting hydrogel, as mechanical strength, structure and degradation rate [53].

3.2.2. Tandem display

Tandem display of proteins or peptides implies the design of a genetic construct with a desired number of protein/peptide repeats intercalated or not by suitable spacers (Figure 3B) [47,53]. Such construct is then translated into a complex protein/peptide display expressed in host cells. The number of repeats as well as the nature of the linker can be varied and tuned depending on the easiness of protein production, namely its solubility and stability. Such modularity allows the easy customization of the final material and its properties. As such, independent parameters including solubility, mechanical properties and/or presence of cellular cues in the final hydrogel can be tuned [53,54]. For example, the peptide module 'RGD' can be introduced in the genetic construct, yielding a display system promoting cell adhesion [9]. This tunability of the building blocks can be designed to interact with cells at different length scales, mimicking more closely their natural environments [55]. On the other hand, peptides can also be introduced in the construct to increase crosslinking and provide mechanical support to the final hydrogel. Another remarkable advantage of this modularity design is the possibility to control the location and density of each functional module [53]. However, no system is perfect and the multivalency of proteins by tandem display also presents some disadvantages. One is related with the fact that expression systems for proteins in tandem present relatively low protein yields (usually lower than 50 mg/l culture), require extensive purification steps and have the risk of endotoxin contamination [18]. If the module is short enough, solid phase peptide synthesis can be an alternative, as peptide synthesizers allow the efficient production of peptides with 30-50 amino acid residues in sub-gram quantities at a reasonable price [56]. Here, it is possible to perform the precise incorporation of desired amino acids, contributing for reproducibility and decreasing polydispersity [57]. Click-chemistry approaches can also be employed to create longer sequences by combining different peptides. Another disadvantage is low mechanical stiffness, which can be improved using composite hybrid hydrogels [58], as described in the third strategy.

3.2.3. Multimeric polymers

Multivalency of the affinity pair components can be achieved by chemical conjugation of the components to branched molecules or polymers (Figure 3C-D). There are several branched molecules and polymers with different configurations, typically star (Figure 3C) or linear branched (Figure 3D). Also, an enormous variety of robust chemistries for conjugation are available, namely COOH- or NH_2-terminated polymers for coupling using carbodiimide crosslinking chemistries, maleimide-terminated polymers for thiol coupling or several click-chemistry tools [33]. The polymers mostly used for these purposes are branched poly(ethylene glycol) (PEG) molecules, which have possess good water and organic solvent solubility, lack of toxicity, rapid clearance from the body and low immunogenicity, similarly to linear PEG [20]. Other polymers have been assessed as poly(propylene oxide), poly(ethylene oxide) diacrylate, N-(2- hydroxypropyl) methacrylamide, polyglycolic acid, polylactic acid and polymer polylactide-co-glycolide [20,59]. Usually the use of polymers for the multimeric display increases the stiffness of the hydrogels structure [19,58]. Moreover, using branched polymers for the coupling of one or both of the components is an easy way to control avidity (combined strength of interactions) [60].

3.3. Applications of affinity-triggered hydrogels

Hydrogels find applications in a myriad of areas, which range from biomedical areas in tissue engineering and repair [61,62], drug delivery or imaging [63,64], to soft robotics [65], wearable electronics [66], sensing [67], soft devices and actuators [68], or power sources [69]. For the particular class of affinity-triggered hydrogels, the examples reported include biomedical uses in the field of tissue engineering and drug release, which will be detailed in this section (Table 3).

Tissue engineering combines biology, engineering and materials science to develop biological substitutes which can improve, restore or maintain tissue function [70]. Independently of cell type, transplantation model or methods of quantification, one of the major issues of tissue engineering is

that only a small fraction of transplanted cells remain at the site after transplantation [24]. As a result, multiple cell injections are required to obtain functional recovery. Encapsulating the cells into a self-supporting material that replicates the *in vivo* cell environment is a good alternative. Using an affinity-triggered hydrogel allows a much better control at the molecular level [53], which is not achieved from materials obtained from natural sources.

Affinity triggered hydrogels have also found applications in drug release. With the appearance of newer and more powerful drugs and slow progress in the efficient treatment of severe diseases, there has been an increasing attention to develop methods of administration of small drugs to larger biological agents into the body [71]. There is a need to improve the efficacy of delivery and controlled release of therapeutics, while lowering dosage and therefore cost of therapy, with simultaneous better patient compliance [48]. The main goals for effective controlled release systems are the controlled location of the payload, the stable release of the therapeutic agent, the lack of toxicity and stability of the entire assembly and encapsulated cargo.

Affinity-triggered hydrogels possess intrinsic properties that make them particularly well suited for these applications (Table 3). Hydrogel stiffness can be controlled by different strategies, including adjustment of polymer concentration, crosslinking method or modulation of the density and distance between crosslinks along the material [72]. Stiffness tuning has also been achieved with affinity-triggered hydrogels, by altering protein concentration [73], the molar ratio of each component [74] and the binding affinity between the components [9]. Stiffness control is a major advantage when working with stem cell differentiation, as it can more closely mimic the *in vivo* environment (Figure 4). Furthermore, as the affinity pairs used typically interact under physiological conditions, hydrogel assembly is made under very mild conditions, perfectly compatible with biological entities as cells or proteins, and also compatible with *in situ* assembly. In addition, it is possible to also disassemble the hydrogel components by adding controlled concentrations of inhibitors or by providing environmental conditions that do not favour binding

between the affinity pair components. On the other hand, and due to the high selectivity that characterizes affinity interactions, it is possible to incorporate chemically or biologically (by genetic encoding) other functional moieties that improve hydrogels performance, namely the introduction of biological cues for cell recognition and control. There are of course some limitations on the use of affinity-triggered hydrogels for tissue engineering and drug delivery. Firstly, each affinity pair has specific properties, namely affinity constant, binding/release conditions, optimal multivalency which requires a case-to-case optimization. Despite the various possibilities to tune hydrogels´ stiffness, their mechanical properties are usually weak. On the other hand, and depending on the availability and easiness of production, the amount and cost of each affinity pair component is varied, and in some cases can be prohibitive for large-scale applications. It is also important to ensure that any new functionality given to the hydrogel through the incorporation of specific functionalities does not interfere with target binding and affinity-pair complex formation due to steric hindrance effects. Finally, binding between the affinity pair components must be assessed in the conditions of the final application, for example in the presence of cell culture media or body fluids, as molecular recognition is context-dependent.

4. Ligand-receptor pairs for affinity-triggered hydrogels and their applications

Over the last 20 years, affinity-triggered hydrogels have gathered the interest of researchers, and several examples have been reported so far. These are summarised in Tables 2 and 4, as well as the main properties and application explored in each case. In this section, the reported examples of affinity-triggered hydrogels will be detailed, and an overview of less traditional approaches will be given at the end.

4.1 Concanavalin and glucose

Lectins are carbohydrate-binding proteins that interact with glycoproteins and glycolipids on the cell surface contribution for cell adhesion and agglutination [75]. Concanavalin is a tetrameric lectin that binds glucose, with an affinity constant of $2x10^4$ M^{-1} [76].

Obaidat *et al* [77] co-polymerized glucose and acrylamide in the presence of initiators. When mixed with commercial concanavalin in the presence of $MnCl_2$ and $CaCl_2$, the physical interactions between both molecules lead to the formation of a self-assembly hydrogel (Figure 5A). The authors observed that a low concentration of glucose-polymer (0.57 mg/ml) and a high concentration of concanavalin (100 mg/ml) was required for hydrogel formation. The hydrogels were sensitive to free glucose, with reversible sol-gel behavior in the presence or absence of glucose. The concentration was dependent on the concentration of glucose-bound polymer. The authors aimed to use this affinity-triggered hydrogel as a self-regulating insulin delivery system, which was achieved in a latter study [78]. The concanavalin/glucose hydrogel was placed between two porous poly(hydroxyethy1 methacrylate) membranes, separating two adjacent chambers. Lysozyme (14.4 kDa) and insulin (5.8 kDa) were added to the first chamber. No protein (lysozyme or insulin) was detected in the second chamber before glucose addition, as the hydrogel did not allow protein diffusion or passage. As the concentration of glucose was increased, the amount of crosslinks decreased and more protein started to be detected in the second chamber (Figure 5B).

Lee and colleagues [79] used a similar strategy to obtain affinity-triggered hydrogels. In their strategy, glucose was co-polymerized with 1-vinyl-2-pyrrolidinone in the presence of initiators. Similarly, when mixed with commercial concanavalin, a hydrogel network was assembled. The authors determined the influence of glucose concentration in copolymer, concentration of glucose to 1-vinyl-2-pyrrolidinone ratio and concentration of concanavalin in hydrogel assembly. The results showed that hydrogel formation was more favorable if the glucose content on the copolymer and/or concentration of concanavalin was increased. The addition of free glucose also resulted in hydrogel dissolution and its removal by dialysis resulted in hydrogel assembly.

A monomer having a pendant glucose moiety has also been used for the formation of concanavalin and glucose affinity-triggered hydrogels [80], with similar response to free glucose and mannose, but not galactose.

4.2.Antibody and antigen

The antibody-antigen interaction has been explored in many areas including therapeutics, diagnosis, *in vitro* analysis and affinity purification [4]. Due to the highly specific and strong interaction, it would be expected that the affinity pair antibody/antigen would be used to assemble affinity-triggered hydrogels. This concept was first explored by Miyata *et al* in 1999 [81]. Rabbit IgG was employed as the antigen and goat anti-rabbit IgG as the antibody, with an affinity constant of $2.6x10^{8}$ M^{-1}. The vinyl-antibody was co-polymerized with acrylamide in the presence of redox initiators and the vinyl-antigen was co-polymerized with acrylamide and N,N-methylenebisacrylamide to allow the multi-display. When both components were mixed, a macroscopic hydrogel network was formed (Figure 6A). The authors observed hydrogel reversible swelling when the hydrogel was immersed in solution containing free antigen and no antigen, respectively. Furthermore, the hydrogel did not swell in the presence of free goat IgG, showing the selectivity of the antibody towards its specific antigen. Further swelling experiments with encapsulated haemoglobin showed that the protein only permeated the hydrogel structure in the presence of rabbit IgG. Such observation renders many possibilities for drug delivery applications [75].

The effect of preparation conditions and network structures on the swelling and shrinking behaviour of the hydrogels was studied [82]. Two different strategies were assessed: (i) both antigen and antibody were chemically coupled to polymers, forming a semi-interpenetrating polymer network (Figure 6A) and (ii) the antigen was immobilized to the polymer chain and the antibody was free, forming antibody-antigen entrapment hydrogels (Figure 6B). The swelling behaviour was strongly

influence by protein concentration and crosslinking density, as well as antigen concentration in the solution. Furthermore, the authors observed that the antibody-antigen entrapment hydrogels did not shrink completely after removal of the antigen, but the semi-interpenetrating polymer network hydrogel did so, with reversible swelling/shrinking behaviour.

Later, Gubeli and collegues [83] explored the affinity of a humanized single-chain antibody fragment with affinity towards fluorescein. Both molecules were conjugated to 40 kDa 8-arm PEG molecules and rendered a G'= 60.5 Pa hydrogel after mixing the two components (Figure 6C). The addition of free fluorescein resulted in total erosion of the hydrogel after 3 hours. The authors assessed the potential of the material for tissue engineering. They observed high human embryonic kidney cell viability after 48 hours. The authors also explored the potential of the hydrogel for vaccination against oncogenic human papilloma virus type 16. They were able to encapsulate capsomeres derived from the viral L1 capsid protein, which was only released after fluorescein addition. The vaccine hydrogel was used to induce the immune response in mice, and observed good tissue compatibility and no significant signs of inflammation or rejection [83].

4.3. Avidin and biotin

Avidin is a natural tetrameric protein that binds biotin with a high affinity constant (10^{15} M^{-1}). Due to its strong affinity, which resembles a covalent bond, the affinity pair has been used for the modification of surfaces, nanoparticles and hydrogels for sensing and drug delivery applications [84–87]. Binding studies with biotin analogues have shown that the main interaction between biotin and avidin is due mostly to the ureido portion of biotin [88]. However this interaction is supported by many contributions. First, there is a shape complementarity between the binding pocket and biotin. Second, an extensive hydrogen bond network is formed between biotin and avidin. The 'first-shell' of hydrogen bonding is made directly with residues located at the binding site (Ser45, Asn49, Ser88, Thr90 and Asp128). A 'second-shell' of hydrogen bonding involves residues that

interact with the former residues [89]. Third, the biotin-binding pocket is hydrophobic, lined with tryptophan residues. Hydrophobic and van der Waals force-mediated contacts further contribute for the high affinity [88]. Furthermore the binding of biotin leads to the stabilization of a flexible loop connecting two neighbor strands of avidin, acting as a 'lid' over the binding pocket and stabilizing the biotin binding [89].

Being one of the most well-known affinity pairs [10], it has been also used for the assembly of affinity-triggered hydrogels. Liu and colleagues [84] modified PEG oligomers with disulphide intra-linkages with biotin on both sides. When mixed with avidin, which has four biotin-binding sites, the authors observed the formation of a macroscopic hydrogel (Figure 7A). When dithiothreitol (DTT) was added to the hydrogel, the intra molecular disulphide bonds where broke and the solution turned liquid and transparent. Although not reported, the authors propose that these hydrogels could be used for drug delivery applications and biomedical treatments, as glutathione is present in the body. Glutathione can reduce disulphide bonds and would cause hydrogel disruption and the release of the encapsulated drug.

Another strategy to assemble avidin/biotin hydrogels was reported by Cui *et al* [90]. Hyaluronic acid was chemically modified with biotin, to generate multivalency, and then mixed with avidin, for hydrogel formation (Figure 7B). When free biotin was added to the system, the hydrogel was dissolved and the solution remained non-viscous. The hydrogel was loaded with an anticancer drug, doxorubicin (DOX), and the release was studied. Although the drug was released from the hydrogel in the presence of buffer solution (60% release after 40 hours), a quicker release rate was observed when the hydrogel was incubated in a solution containing free biotin (90% after 40 hours).

In another example, a linear maleimide-terminated PEG molecule was modified with biotin for multivalency [10]. When mixed with avidin, a hydrogel was formed. Gel erosion was measured by using fluorescently-labelled streptavidin, with stability observed for over 9 months, though tunable between five days to three weeks depending on gel concentration. They also observed immediate

complete erosion when free biotin was added. This system was used for human mesenchymal stromal cells encapsulation. For this purpose, biotin was conjugated to two different peptides, one with the cell adhesion motif (RGDS) and a second with the cell adhesion motif and a matrix-metalloproteinase (MMP) cleavable sequence (PQG↑IWGQ). The fast gelation and the strong network allowed a homogeneous dispersion of cells through the hydrogel matrix. A high cell survival was observed after 24 hours (95.4 %), indicating the nontoxicity of the hydrogel and its suitability for cell culture applications. Hydrogel containing higher concentrations of the PEG functionalized with biotin-MMP resulted in significantly larger cell spreading.

More recently, our group explored the avidin/biotin affinity pair in a rational approach towards affinity-triggered hydrogels with tunable properties [91]. The influence of multimerization (linear, 4-arm and 8-arm) on the erosion and stiffness of the hydrogels was assessed in view of the binding constants. A higher binding affinity was observed between avidin and multimeric biotin conjugated to 4-arm PEG (in comparison to 2-arm and 8-arm multimerization strategies), pointing to a better molecular fit between the two components. This was also observed in the mechanical properties - hydrogels formed by avidin/4-arm PEG-biotin (Figure 7C) were more robust than avidin/8-arm PEG-biotin (Figure 7D) – and in the erosion profile - avidin/4-arm PEG-biotin hydrogels were stable for 3 months versus 5 hours for avidin/8-arm PEG-biotin (Figure 7E). Biotin conjugated to linear PEG did not yield a self-supporting network. Higher concentrations of avidin/4-arm PEG-biotin resulted in stiffer hydrogels (higher G´) but had no major influence in erosion. The avidin/4-arm PEG-biotin hydrogels were biocompatible and further used to encapsulate induced pluripotent stem cells and support their differentiation into a neural lineage. After 14 days, the expression of PAX6 (transcription factor for ectoderm specification) and Nestin (a filament protein expressed in cells from the central nervous system) were visible by immunochemistry, and the presence of SOX2 and Z01 was consistent with the formation of neuro-epithelial rosettes (Figure 7F).

4.4. Heparin and heparin-binding molecules

Heparin is a naturally occurring anticoagulant and has shown the ability to sequester and stabilize growth factors, making it an interesting molecule to explore in affinity-triggered scaffolds for cell-related applications. Heparin is known to bind to residues 111-165 of the C-terminal of vascular endothelial growth factor (VEGF), where the carboxylate groups, 2-O-, 6-O- and N-sulfation groups of heparin contributing for this interaction [92]. Yamaguchi *et al* [73] explored the affinity pair for hydrogel formation. Commercial heparin was combined to a four-arm branched PEG molecule via thiol chemistry. Dimeric VEGF was produced in *E. coli,* purified by heparin-affinity chromatography, and used without any further conjugation. When both components were mixed, they formed a self-supporting viscoelastic hydrogel for VEGF delivery (Figure 8A). The affinity constant between VEGF and heparin is $6x10^6$ M^{-1} [93] and the resulting affinity-triggered hydrogel displayed a weak viscoelastic behavior (G'>10 Pa). These hydrogels have found applications in drug delivery, as heparin is naturally occurring anticoagulant and has the ability to sequester and stabilize growth factors. In the presence of VEGF receptors, the crosslinks were selectively destroyed, and hydrogel erosion was observed (after 4 days) as well as release of radioactive labelled VEGF (nearly 80 %). The released VEGF still displayed bioactivity, contributing for an increase of the proliferation of porcine aortic endothelial cells, compared to the control. Combined with their ability to release VEGF, the hydrogels promoted vascularization. Although these hydrogels were not being studied for tissue engineering applications, it is possible to infer about their suitability for this application based on their properties.

Other heparin binders, namely small peptides, are described in the literature. The heparin-binding domain of heparin interacting protein (HIP), with the sequence CRPKAKAKAKAKDQTK, has been reported to bind non-specifically to glycosaminoglycans [92] and the peptide $PF4_{ZIP}$ (CGGRMKQLEDKVKKLLKKNYHLENEVARLKKLVG) is a coiled-coil heparin-binding peptide modelled from a heparin-binding domain of human platelet factor, where lysine residues

play an important role in the binding mechanism [74]. The affinity pairs heparin/HIP [51] and heparin/$PF4_{ZIP}$ [74] have been used for the development of affinity-triggered hydrogels (Figure 8B). In both works, both components (low molecular weight heparin and the heparin-binding peptides) were conjugated to four-arm star PEG molecules and formed a hydrogel when mixed at room temperature. The affinity between $PF4_{ZIP}$ and heparin (approximately 10^5 M^{-1}) was not temperature-dependent, and hydrogels presented consistent mechanical properties from 5°C to 37°C. These authors, as many others, also observed that the mechanical properties are greatly influenced by the concentration and molar ratio of both components. As expected, an increase on the molar ratio of the peptide results in an increase of the storage modulus, with a maximum of G'= 180 Pa. As the affinity pair heparin/$PF4_{ZIP}$ has a lower affinity compared to the affinity pair heparin/VEGF, the increase of the storage modulus is most likely a consequence of the heparin/$PF4_{ZIP}$ hydrogel using a branched PEG molecule for the display of both components. The hydrogels formed on the basis of the interaction between peptides and heparin found applications in drug delivery with the controlled release of basic fibroblast growth factor (bFGF) from heparin/HIP hydrogels [51]. The bFGF solution was encapsulated within the hydrogel, without network disruption. The bFGF and the HIP binding sequences to heparin are reported to be different; therefore bFGF does not compete to the same binding site as HIP. In this study, the hydrogel presented 16.8 % of weight loss and 16.1 % of bFGF release after 4 days. The release of VEGF referred in the first example was much faster, as VEGF contributed for the physical crosslinks of the hydrogels itself; in this case bFGF was encapsulated within the network and its release was driven mainly by diffusion. This suggests that if the hydrogel is to be used for a long term therapeutic application and the release of the bioactive molecule should be slower, the molecule itself should be encapsulated and not be participating in the formation of the physical network. On the other hand, Zhang *et al* [74] explored the release of bFGF from heparin/$PF4_{ZIP}$ hydrogels. The authors observed a burst release in the beginning and a linear slow release for the next 10 days. It is important to stress that the release is always due to

hydrogel erosion. After 8 days the authors observed a direct correlation between hydrogel erosion and bFGF release. Although no application in tissue engineering has been described yet, the peptide-heparin gels display storage modulus values compatible with cell encapsulation – the literature estimates a minimum requirement of 50-100 Pa to allow mammalian cells suspension for tissue engineering applications [94]. Combined with their ability to release basic fibroblast growth factor they could aid in vascularization processes.

Other authors used the heparin binding peptide PBD1, with the sequence KAFAKLAARLYRKAGC. It displayed the highest affinity towards heparin ($3.3x10^7\ M^{-1}$) (Figure 8D) [95]. The authors describe shear-thinning hydrogels that were able to sequester exogenous heparin-binding peptides and release them based on their dissociation constant towards heparin. Peptides with lower affinity towards heparin were released at a quicker rate compared to peptides with a higher affinity towards heparin. The authors have also reported a dependence of the mechanical properties on temperature [96]. The same hydrogel displayed a storage modulus 10-times higher at 4ºC (5000 Pa) than at 45ºC (480 Pa). This can be explained by lower diffusion coefficients and kinetic rate constant that result in increased time of contact between the affinity pair at lower temperatures. The cargo was release after 3 days, with 100 % of the hydrogel eroded. This feature is important for drug delivery applications, as the hydrogel network can be formed at lower temperatures and it will only release its encapsulated cargo when exposed to higher temperatures (e.g. body temperature). Although the gelation time of these hydrogels is within range of other described affinity-triggered hydrogels, their temperature-dependent behaviour can compromise their use in tissue engineering applications, in particular, in cell encapsulation.

Later, the same authors explored the same affinity system with different heparin-binding peptides [96]. The two heparin-binding peptides derived from antitrombin III (dG, dansyl-GKAFAKLAARLYRKAGC, and W, WKAFAKLAARLYRKAGC) displayed different affinities towards heparin and observed different viscoelastic properties. The peptides described have a

shielded hydrophobic core by positively-charged amino acids that contribute for solubility of the peptide and affinity towards anionic heparin. The authors increased the complexity of the system by including a cross-linker peptide with cysteine residues (GCRGDSGPQGIAGQGC) that stabilized the hydrogel network by chemical crosslinking with the free vinyl sulfone moieties of the PEG molecule (Figure 8D). The hydrogel, which included in its composition the weakest affinity pair displayed a lower storage modulus (G'= 1060 Pa) compared to the hydrogel which included in its composition the strongest affinity pair (G'= 2760 Pa), as well as a lower time of gelation (27 minutes and 7.3 minutes, respectively). This reveals the importance of the affinity constant between the pair for the formation of hydrogels with different mechanical properties. Although these hydrogels were not described for any particular applications, they show promising storage modulus for cells that require stiffer supports.

4.5. TIP1 and TIP1-binding peptides

The Tax-interacting protein-1 (TIP1) is composed by a PDZ domain, a protein-protein interaction domain with a key role in cellular signalling, and a possible target for drug design [97]. The general recognition mechanism between TIP1 and TIP1-peptide ligands is based on the hydrophobicity character of the binding pocket of PDZ domains as well as a structural glycine to form hydrogen bonds between the C-terminal carboxylate of the ligand and the protein backbone amides. The C-terminal amino acids of the peptide ligands tend to form β-sheet interactions with β2 strand of TIP1 [97,98].

Ito *et al* [11] developed a hydrogel based on TIP1 and its β-catenin analogue peptide ligand (CQLAWFDTDL). The first component (TIP1) was fused to a stable trimeric protein (CutA) to allow a trimeric display. The second component (TIP1-recognizing peptide) was fused to a four-arm PEG molecule (Figure 9A). The affinity pair presents an affinity constant of 2.3×10^6 M^{-1}. By mixing the two components, the authors were able to form a spontaneous viscoelastic hydrogel with

shear-stress behaviour and reversible-phase transformation. The authors studied the applicability of the hydrogels for cartilage tissue engineering. Chondrocytes were encapsulate within RGD-containing hydrogels, while still observing spontaneous gelation. Cells were still viable after 8 days of culture, as determined by the live-dead assay. The authors have also demonstrated the importance of the RGD motif, as matrices without the RGD motif did not support cell proliferation.

Guan *et al* [99] increased the complexity of the system by adding a SH3-recognizing domain (called docking station peptide) fused to the TIP1. This docking station peptide allows the functionalization of the network with SH3-tagged proteins (Figure 9B). These constructs were able to form hydrogels with a storage modulus of 262 Pa, which displayed self-healing properties and were explored for drug delivery applications. Two fluorescent molecules were encapsulated in the matrix and a faster release rate of the smallest molecules (20 kDa dextran versus 524 Da pyranine) was observed. It was also possible to immobilize globular proteins by fusing a docking station-tag to two different proteins (green fluorescent protein and laccase). Hydrogels with immobilized laccase were more stable as the protein is a trimer and can further contribute to increase the crosslinking of the hydrogel network. A release of protein by means of hydrogel erosion was recorded. This principle could be used for other bioactive molecules or drugs.

Other authors have used an ubiquitin-like domain (ULD) as the tetrameric display domain of the TIP1 protein [100] (Figure 9C). Although a direct comparison is not possible, the ULD display should render hydrogels with a higher stability than the CutA display, due to the higher number of possible crosslinks in the tetrameric display. Mesenchymal stem cells were encapsulated, achieving high density and viability after 7 days. The authors were able to have an increase of the metabolic activity of 359 % at day 7.

In the literature several TIP1-binding peptides have been described with different affinities towards TIP1, which can still be explored for the formation of hydrogel with different properties. For example, by studying the molecular interactions between TIP1 and a natural peptide ligand (Ka =

$1.6x10^5$ M^{-1}), it was possible to define a peptide motif (WRESAI) with a higher affinity towards TIP1 (Ka = $1.2x10^8$ M^{-1}).[98] This tight binder was then fused to a self-assembly motif (Nap-GFFYGGWRESAI) which formed nanofibers in solution, resulting in a viscous solution.[101] The network was further enhanced when the self-assembly peptide was mixed with ULD-TIP1 (maximum of 320 Pa of mechanical strength). The affinity-triggered interactions were used to further increase the mechanical stability of the previous system, and peptides with different affinities towards TIP1 resulted in hydrogels with different mechanical properties. Although these hydrogels were not described for any particular application, it is possible to conclude that it has an adequate storage modulus to support cell encapsulation.

A different multimerization domain for TIP1 was reported by Zhang and colleagues.[102] A hetero-hexameric protein system composed by three ubiquitin-like self-assembly domains was employed. As the second component the peptide Nap-GFFYGGWRESAI was used as the second component, taking advantage of the self-assembly properties and the high affinity towards TIP1. The storage modulus depended on the number of TIP1 molecules, with gel formed by the complex with six TIP1 molecules (6T) registering the highest value, due to a higher crosslinking density. By examining the size of the nanofibers by TEM, an increase of the nanofiber diameter (initially 35 nm) after the addition of the TIP1 complex was observed. A significant increase of the fiber diameter (from 38.5 nm to 60.3 nm) with an increasing concentration of TIP1 complex (from 0.05 wt % to 0.4 %) was also verified and directly correlated with the mechanical properties (20 Pa to 100 Pa, respectively). This work also demonstrated that the mechanical stiffness of the gel can be tuned by changing protein concentration, peptide concentration and the number of TIP1 binding sites. The hexameric protein which allowed the multi-display of TIP1 was further engineered to include a recombinant pneumococcal cell-wall amidase LytA. When mixed with the self-assembly peptide binder, the authors were able to obtain a stable hydrogel. LytA binds a dye-peptide conjugate (Rhoda-GGK), which was used as a model to test the potential of the hydrogel for drug

release. A controlled and sustainable release of the Rhoda-peptide was observed. Additionally, the concentration of 4T2C (fusion protein composed by four TIP1 units and two LytA) influenced the release profile of Rhoda-peptide, with higher protein concentrations leading to slower release rates. A higher concentration of 4T2C will translate into more possible binding sites for Rhoda-GGK, decreasing the amount of dye that diffuses out of gel in the same time length. However, the release behaviour is much faster than the release behaviour of the previous system described (hours versus days). This may be mainly explained by the lower affinity between LytA/Rhoda-peptide in comparison to the affinity between heparin/heparin-binding peptides. Still, if a specific application requires a rapid release of a therapeutic drug, this system is still suitable. Although this hydrogel was not studied for tissue engineering applications, the authors describe a quick recovery after removal of an external stress (600 seconds). Though not as fast as other systems described herein, the hydrogels still exhibit shear-thinning properties and could be used as an injectable to support cell growth. However the immunogenicity of LytA would have to be previously studied.

4.6. Docking and Dimerization Domain and Anchoring Domain

The self-assembling Dock-and-Lock system relies on protein-protein interactions which were explored for hydrogel formation. In these materials, the first component is a docking and dimerization domain derived from cAMP-dependent protein kinase A. The second component is the anchoring domain of A-kinase anchoring proteins [103]. The docking and dimerization components form a type-X four helix dimer with nanomolar affinity towards the α-helical amphipathic anchoring domain [104], which non-covalently "locks" the dimer from disrupting (Figure 10A). This interaction is mainly due to the aliphatic residues of the docking and dimerization domain and the predominantly hydrophobic interface of the anchoring protein [104]. Lu *et al* [103] have used this pair for the formation of engineered protein-based hydrogels (Figure 10B). The authors engineered the docking and dimerization domain to be linked by a random-coil spacer with "RGD"

sites and the anchoring domain was conjugated to four-arm and eight-arm PEG molecules. Due to the low solubility of the anchoring domain, the authors engineered the sequence to include a peptide that would contribute for the solubility by increasing the net charge. The authors observed an increase of the mechanical stiffness with an increase of the concentration of the components, with a 100-fold improvement of the storage modulus when the concentration changed from 5 wt % to 10 wt %. Increasing the PEG-arm valency from four to eight led to an increase of hydrogel storage modulus (100 Pa to 300 Pa). The hydrogel was used as a vehicle to encapsulate mesenchymal stem cells, which exhibited high cell viability after injection through a 21-gauge needle and after 3 days of culture. These hydrogels were able to sustain very large strains before yielding, with values 1-2 orders of magnitude higher than other shear-thinning hydrogels. After removing the deformation stress, the fractured hydrogel very rapidly recovered back into gel form very fast, within 6 seconds. This is an important property if the gel is to be used in regenerative medicine applications and to ensure cell encapsulation at the site where it will be injected. The authors also showed to be promising for drug delivery applications due to its erosion profile. The physical cross-linked hydrogel showed an initial high erosion, followed by slower and linear erosion rate (Figure 10C) [103]. The erosion rate was slower when compared with other affinity-triggered hydrogels. It was also possible to tune the erosion rate. Increasing the multivalency of the PEG molecule decreased the erosion rate - the gel composed by the 4-arm PEG eroded 90 % after 5 days compared to 15 days for the hydrogels composed by the 8-arm PEG.

Later, this system was combined with the photo-chemical cross linker methacrylate to produce hydrogels with higher rigidity (10-fold) [105]. This modification allows the components to be chemically crosslinked via light initiated radical polymerization, and it can be controlled by adjusting light exposure time, intensity and initiator concentration. Here, the anchoring domain and the methacrylate crosslinking were conjugated to a linear hyaluronic acid polymer instead of a PEG multi-arm molecule. The methacrylate did not interfere with the shear-thinning and self-healing

properties of the hydrogel and contributed for the viability of encapsulated mesenchymal stem cells, with an increase compared to the physically-cross-linked system (98 % versus 73 %). This can result from increased hydrogel stability or preference of mesenchymal stem cells for stiffer scaffolds. Regarding drug delivery applications, only 10% erosion was observed after the two first weeks and negligible erosion rates for over two months (Figure 10D). If the hydrogel was incubated with a solution of hyaluronidase, the hydrogel eroded. The erosion rate of this type of hydrogel can be tuned for the therapeutic application in vision. If a burst of the therapeutic drug is intended, a hydrogel with a faster erosion rate can be employed. If a long and slow release of a therapeutic drug is intended, a chemically crosslinked hydrogel with a slower erosion rate can be used. If a sudden release is necessary hyaluronidase can be injected and induce complete hydrogel erosion and drug release. The interaction between these two domains has extensively been studied and there is available a library of complementary domains [106] that can be engineered into affinity-triggered hydrogels with different properties.

4.7. Calmodulin and calmodulin binding domains

Calmodulin is an important regulator of many Ca^{2+} sensitive pathways, and calmodulin-binding domains present affinities spanning 5-orders of magnitude and varying Ca^{2+}-dependencies. Topp *et al* [107] explored the affinity between calmodulin and two calmodulin-binding domains: endothelial NO synthase (eNOS) with Ka = $3.3x10^8$ M^{-1}, and petunia glutamate decarboxylase (PGD) with Ka = $5.0x10^7$ M^{-1}. The eNOS domain binds in an antiparallel orientation to calmodulin by extensive hydrophobic interaction [108], whereas PGD forms a self-dimer and shares both hydrophobic and electrostatic interactions with calmodulin [109]. By taking advantage of the natural affinity between these molecules, the authors created a genetic toolbox for the formation of physically-crosslinked hydrogels (Figure 11). Branching was provided by a bivalent hydrophilic linker (the peptide $(AG)_3(PEG)_n$, n = 8, 40). A leucine zipper self-assembly domain, which forms a tetrameric bundle,

was included for increased crosslinking. The hydrogel formation is dependent on the presence of Ca^{2+}, which binds to calmodulin rendering it active. Upon mixing the two components the solution remained non-viscous; after Ca^{2+} addition the viscosity increased 5000-fold leading to the formation of a hydrogel. Addition of EDTA disrupted the network by Ca^{2+} chelation. The influence of other metals was also studied - when Ca^{2+} was substituted by Mg^{2+} a 3-fold increase of viscosity was observed, reflecting the selectivity of calmodulin to specific ions. Although this system was not described for a specific application, it is possible to find it suitable for drug delivery applications. If a drug was encapsulated within the hydrogel network it could be delivered to the target place. Without data about diffusion, pore size or hydrogel erosion, it is not possible to conclude about the release behaviour of an encapsulated drug. However, if a burst release was necessary, a local injection of Ca^{2+} would cause the hydrogel to disrupt its network and deliver the encapsulated therapeutic drug. Nonetheless, further research with the system should be performed before taking further conclusions or making comparisons with other described affinity-triggered systems. The system described also offers some advantages, such as the possibility of controlling pore size, by genetically controlling the length of the hydrophilic linkers.

4.8. WW domains and proline-rich peptides

The WW domain is a 31-40 amino acid sequence with two conserved tryptophan (W) residues spaced by 20-22 amino acids [110], which can be found in more than 200 multidomain proteins and is responsible for mediating various protein interactions. WW domains are located in the recognition region of these proteins and bind to proline-rich peptides, triggering changes in the cellular environment and signalling pathways [111]. Heilshorn's group has explored the natural interaction between WW domains and proline-rich peptides to form so called mixing-induced two component hydrogels (MITCH). The MITCHs were first described by Foo *et al* [9] and are composed by a tandem WW domain linked by a hydrophilic spacer containing 'RGD' modules, and

a tandem proline-rich domain linked by a hydrophilic spacer ((AGAGAGPEG)$_2$) (Figure 12A). Due to their natural molecular recognition, the components assemble into a hydrogel when mixed at physiological conditions, without the need of any external stimulus. Several of these MITCHs have been reported. Foo *et al* [9] studied two WW domain tandem modules with different affinity towards the proline-rich peptide – the natural WW peptide Nedd4.3 (Ka = 1.6x10^4 M^{-1}); a computer-derived WW peptide CC43 (Ka = 2.2x10^5 M^{-1}) - resulting in hydrogels with different stiffness. The WW domain with the weakest affinity constant towards the proline-rich peptide resulted in a softer matrix (G'= 9 Pa) compared to the WW domain with the highest affinity (G'= 50 Pa). The importance of avidity was demonstrated by changing the number of crosslinks, herein given by the number of repeats within the tandem protein – a hydrogel was only formed when 7 repeats of WW and 9 repeats of proline-rich peptide were mixed; the solution remained non-viscous when 3 repeats were mixed. The hydrogel was used as a 2D and 3D support for cell proliferation and differentiation. Films were shown to be cell compatible and allowed self-renew and differentiation of neuronal-like PC-12 cell line and dissociated murine adult neural stem cells (NSCs), as cells adopted typical neural morphologies after differentiation. Three cell culture types were successfully encapsulated within 3D matrices: PC-12 cells, human umbilical vein endothelial cells (HUVECs), and murine adult NSCs; all remained viable after 5 days of 3D culture. The hydrogel was also capable of supporting differentiation of adult NSCs, with neuronal MAP2-positive and glial GFAP-positive cells encapsulated within the hydrogel. Multiple elongated neurites extending in all three directions were observable (Figure 12B). The self-healing properties of the hydrogels was also assessed, with self-healing occurring in 5 minutes and 30 minutes for the hydrogel composed by the strongest (Ka = 2.2x10^5 M^{-1}) and weakest affinity pair (Ka = 1.6x10^4 M^{-1}), respectively. Only the strongest affinity pair renders a promising hydrogel for cell encapsulation and delivery, as 30 minutes to regenerate is too long and most cells would be lost before hydrogel self-assembly. Furthermore, at room temperature, the weakest binding pair (Ned4.3 and proline-rich

peptide) formed a hydrogel with a storage modulus of 9 Pa, similar to 50 % Matrigel; and the strongest binding pair (CC43 and proline-rich peptide) formed a hydrogel with a storage modulus of 50 Pa, similar to 100 % Matrigel [9]. The former data demonstrates that the viscoelastic properties of the MITCH materials are within the appropriate range to be used as ECM-mimics and contribute for a better understanding of cell behaviour. The same system was used to access the viability of encapsulated adipose-derived stem cells, with over 90% viability after 10 days,[25] as well as the *in vivo* injection into nude mice, with viable cells at the injection site after 10 days. Another example included the encapsulation of the VEGF-mimetic peptide QK-fused to one or two-proline-rich peptide repeats [112]. By using fluorescence recovery after photobleaching (FRAP), the diffusion of fluorescently labelled QK and QK-fused to proline-rich peptides was studied. The diffusion of the peptide was higher for free QK, followed by QK-fused to one repeat and QK-fused to two repeats. The conjugation of QK to the proline-rich peptides slowed the mobility of QK through the hydrogel and a higher avidity resulted in slower molecule mobility. Showing capacity to bind to VEGF receptors, its capacity to activate endothelial cell migration and network formation was assessed. Performing an *in vitro* scratch wound healing assay, human umbilical vein endothelial cells treated with QK showed slower wound closure (56.3 % at 12 hours) compared to cells treated with QK-fused to one and two repeats of the proline-rich peptide (66 % and 62 %, respectively). Furthermore, human umbilical vein endothelial cells spheroids were encapsulated in a matrix of collagen type I and fibronectin and MITCH containing the QK-conjugates were injected in the centre, stimulating significantly higher outgrowth, suggesting prolonged drug retention and slow release of QK.

The same affinity pair has also been multi-displayed using PEG, where the WW domain was presented in tandem and the proline-rich peptide was combined to an eight-arm PEG molecule (Figure 12C) [113]. When the proline-rich peptide was conjugated to a four-arm PEG and mixed with the tandem counter partner (7 repeats), no hydrogel formation was observed. The effect of

avidity was tested, by varying the number of repeats of the proline-rich peptide attached to the PEG molecule (one or two), and the effect of polymer weight, by varying the molecular mass of the eight-arm polymer (20 kDa or 40 kDa). Decreasing the PEG molecular weight or increasing the avidity resulted in stiffer hydrogels, with the hydrogel formed by two proline-rich peptides conjugated to 20 kDa eight-arm PEG and the tandem WW exhibiting the highest storage moduli. Hydrogels displayed self-thinning and self-healing properties besides the low mechanical stiffness. The ability to release VEGF and its influence of cell viability was also assessed when the proline-rich peptide was conjugated to an eight-arm PEG molecule [113]. The molecule showed lower mobility within stiffer hydrogels – the slowest diffusion rate was recorded for hydrogels composed by eight-arm PEG with a weight of 20 kDa and functionalized with two repeats of proline-rich peptide. Stiffer hydrogels also took longer to erode, making it a better candidate for drug release applications which require a slower release rate. Encapsulation of pluripotent stem cell-derived endothelial cells within the stiff hydrogel (hydrogels composed by eight-arm PEG with a weight of 20 kDa and functionalized with two repeats of proline-rich peptide) and delivered through a 28-gauge needle showed no loss of cell viability. The co-delivery of pluripotent stem cell-derived endothelial cells and VEGF encapsulated in the hydrogel formulations improved tissue regeneration and reduced necrosis compared to the controls (Figure 12D). Although the low mechanical stiffness of the previous hydrogels is an advantage for the development of shear-thinning injectable hydrogels, its rapid degradation can be a disadvantage for long-term cell survival.

To address this issue Cai *et al* [24] combined the WW domain/proline-rich peptide affinity pair with the hydrophilic polymer PEG and the thermo-responsive polymer poly(N-isopropylacrylamide) (PNIPAM). The authors were able to reinforce the hydrogels network by using two different physical crosslinking mechanisms, resulting in a hydrogel with storage shear modulus 10-times higher than the single network hydrogels described before (G'= 100 Pa). By varying the ratios of the different components, the authors were able to tailor the stiffness of the resulting hydrogels.

These hydrogels displayed rapid and reversible self-healing (< 2 seconds), which is quicker than the previous reported examples, making it a very promising candidate for injectable applications. Human adipose-derived stem cells were successfully encapsulated within the hydrogel and injected through a 28-gauge syringe, with a viability of 93 % versus a viability of only 69 % when injected within phosphate-buffer solution. Cell transplantation efficiency was also tested *in vivo*, by injecting the encapsulated cell into nude mice (Figure 12E). After 3 days, 70 % was possible in comparison to 30 % for the single physical-crosslinked hydrogel, with an increased number of metabolic active cells after 14 days. This increase can be due to lower cell apoptosis decreased cell migration from the injection site and/or enhanced cell proliferation. The increased retention of cells at the injection site is a major advantage of these hydrogels for regenerative medicine applications. The authors also studied the diffusivity of a 40 kDa dextran using FRAP. By increasing the PNIPAM secondary network from 0 to 0.7 to 1 wt %, the authors observed a significant decrease in the diffusion rate. As diffusion is correlated with mesh size, the higher concentration of PNIPAM may have resulted in smaller pores, decreasing the diffusion rate of dextran. Furthermore the erosion behaviour was also studied, with a lower erosion rate being observed for hydrogels with a higher PNIPAM content (Figure 12F).

Mulyasasmita and colleagues [114] have studied the hydrogels composed by WW-domain and proline-rich peptide, using a combination of protein science methodologies and a simple polymer physics model to predict the effect of polypeptide binding interactions on network crosslinking density, sol-gel phase behaviour and gel mechanics. Methodologies included particle tracking microrheology, bulk rheology, dynamic light scattering, circular dichroism and isothermal titration calorimetry.

Recently our group has studied the interaction between a shorter version of a WW and the peptide PPxY [115]. The shorter WW version was obtained by chemical synthesis, a more rapid and less complex way of manufacturing small peptides. Both peptides were conjugated to multimeric PEG

molecules, and their interaction was confirmed both by computational and experimental studies. When mixed together, an affinity-triggered hydrogel was formed. Although using a smaller version of WW, the measured affinity and storage modulus were within the same order of magnitude as in previous works using the entire domain.

4.9. Tetratricopeptide repeat domains and peptide ligands

The 34 amino acid tetratricopeptide repeat (TPR) (Figure 13A) naturally occurs in tandem repeat arrays and is involved in the assembly of multi-protein complexes, like heat shock protein-based multi-chaperone machinery [116]. The TPR units can be manipulated and engineered to bind different peptide ligands. Grove *et al* [94] explored this tandem display where one of the components was a repeat module of the helix-turn-helix tetratricopeptide binding motif and spacer, and the second was a peptide ligand (CGYGGDESVD) conjugated to a four-arm PEG molecule (Figure 13A). The kinetic of gel formation depended on the concentration of the components (from a minimum of 1 wt %), the ratio of TPR units to peptide ligand (a minimum ratio of 1:2), and solution conditions (e.g salt concentration). The hydrogel reported showed a storage modulus of 270 Pa. The interaction between the TPR unit and the peptide ligand was mainly electrostatic and its strength decreases as the ionic strength increases – the affinity constant is $2x10^5$ M^{-1} in the presence of 10 mM NaCl and $3x10^4$ M^{-1} in 500 mM NaCl. This can be useful to induce gel erosion in high salt environments. This hydrogel was studied for drug delivery applications. As the interaction is mainly electrostatic, it can be tailored by changing the ionic strength [94]. Increasing the ionic strength from 10 mM to 500 mM led to hydrogel erosion, making it suitable for drug delivery applications – although it can be discussed if 500 mM salt would not be too high to allow cell survival. By tuning the ionic strength of the medium, it was possible to observe different release profile of the molecule rhodamine (Figure 13B) and of a model fluorescent protein. Rhodamine, as

a smaller molecule (479 g/mol), was released 10-times faster than the fluorescent protein (26,000 g/mol).

The system was further improved by combining different peptide-binding modules, spacer modules, peptides and display approaches. The different combinations resulted in different crosslinking geometry and network stability, resulting in hydrogels with different properties [117]. The release behaviour of 1,6-dimethyl-3- propylpyrimido[5,4-e][1,2,4]triazine-5,7-dione (commonly known as C9, an anticancer compound) was also assessed (Figure 13C), which was slowly and continuously released from the hydrogels over a period of 24 hours. The authors also studied the release of the anticancer compound encapsulated within the hydrogel into a culture of HER2-positive BT-474 breast cancer cells. The hydrogel itself was cyto-compatible, not interfering with cell adhesion. Meanwhile, the anticancer compound released from the hydrogels caused cell death and only cell debris were visible, supporting the release of active compound to the culture. Although these hydrogels were not described for tissue engineering application, they display a suitable storage modulus (270 Pa) to allow mammalian cell encapsulation. Due to the physical nature of their crosslinks the hydrogels most likely display shear-thinning properties, allowing for the local injection of cells and further hydrogel formation and enhanced cell retention at the damaged location.

4.10. Bacterial gyrase subunit B and coumermycin

Ehrbar and colleagues [118] explored the affinity of a bacterial gyrase subunit B towards the antibiotic coumermycin (Ka= 10^8 M^{-1}). A histidine-tagged bacterial gyrase was grafted on a polyacrylamide network via the chelator nitrilotriacetic acid (NTA) charged with Ni^{2+}. Coumermycin was dimerized by the bifunctional crosslinking agent dimethylsuberimidate. With a concentration of 6 %, when mixed together, a self-assembly hydrogel was formed (Figure 14), with a G'= 248 Pa. A low erosion (13 %) was observed after 12 hours. When the hydrogel was mixed

with monovalent novobicin, the hydrogel would disrupt due to competition towards the gyrase binding sites, with 100 % erosion observed after 11 hours. The degradation rate was dependent on novobiocin concentration, with a higher rate observed when the hydrogel was incubated with a higher concentration of the competing molecule. The affinity-triggered hydrogel was used for VEGF delivery. The release could be tuned in a novobiocin concentration-dependent manner. It also allowed the survival of human embryonic kidney cells, with no visible cytotoxic effect. Encapsulated human umbilical vein endothelial cells were viable after 96 hours. Furthermore, the controlled release of VEGF contributed for cell proliferation compared to controls without encapsulated VEGF.

5. Challenges and future prospects

Affinity-triggered hydrogels are promising biomaterials at the interface of materials science and protein engineering. They rely on reversible, specific non-covalent and tunable interactions between components bearing ligand-receptor pairs displayed in a multivalent manner. The driving force for hydrogel assembly is the net of weak non-covalent interactions, which contributes for the gelation process to occur under mild conditions that promote molecular recognition.

A wide range of ligand-receptor pairs is described in Biology representing a toolbox yet to be explored to tailor hydrogels´ properties. Examples of affinity-triggered hydrogels reported so far explore mostly natural affinity partners, but there are several tools in hand to manipulate the affinity and selectivity of the interaction between ligands and receptors, including computational design [9] or protein engineering tools, using for instance display technologies [119]. Proteins and peptides can also incorporate non-canonical amino acids (by synthetic or biological means) in order to uncover new functions. A second level of tunability in affinity-triggered hydrogels relates to the multivalent display of the ligand-receptor components. Such multivalency can be achieved simply by using natural multimeric proteins, or by applying biological and chemical tools to display

proteins in tandem or to covalently couple proteins to branched polymers, respectively. In this context, the environment created by the multivalent display will interfere with the interaction between ligand and receptor, as the two entities will feel stereochemical hindrance, solvation effects and the presence of the moieties used to create the multivalency. Furthermore, depending on the final application of the hydrogels, the media in which they are formed also plays a role in the affinity and selectivity between the hydrogel components. A third level of tunability in affinity-triggered hydrogels is given by the potential to introduce other chemical functionalities, molecular entities (e.g. bioactive peptides), or micro- and nanostructures, which will influence the function of the materials. Taken together, all these aspects contribute to the mechanical, morphological and functional properties of the hydrogels [48]. The *de novo* design and control of affinity-triggered hydrogels is a complex and challenging task, derived from the multitude of modular units available to create the materials. A recent study [120] provides an interesting insight about the design by principle of affinity-triggered hydrogels with desired mechanical properties. A correlation is made between the mechanical properties of the hydrogels and the nanomechanics of the hydrogel components, which may prove in the future useful to design new affinity-triggered hydrogels.

Affinity-triggered materials typically lack mechanical stiffness. A way to increase the mechanical properties relies on the introduction of additional synthetic polymers and crosslinking methods to the multicomponent affinity-triggered system. Inspired in the responsive hydrogels, affinity-triggered hydrogels can be developed to be sensitive to several stimuli. WW/proline-rich peptides hydrogels were combined with the thermo-responsive polymer PNIPAM contributing to an increased mechanical stiffness and a temperature-dependent behavior [24]. The hydrogel can have a modular nature and natural and engineered materials can be combined in order to obtain the desired response, with the possibility of developing multi-responsive hydrogels. For example, Huang and colleagues developed a hydrogel that has a dual response to pH and temperature with enhanced mechanical properties [121]. The topic of responsive hydrogels has been extensively reviewed

[122,123] and can serve as an inspiration to develop responsive affinity-triggered hydrogels. Light is a particularly interesting stimulus to assemble hydrogels as it allows the precise control over temporal and spatial signals, and the topic has been extensively reviewed elsewhere [124–127]. Response to pH could benefit drug release applications – e.g. the low pH of the digestive tract would influence material degradation and allow the release of the encapsulated drug [128]. Next-generation affinity-triggered hydrogels may even be prepared to react to cell-secreted biological inputs in a way that mimics the dynamic environment of the ECM, actively contributing to tissue development and regeneration [129]. As a starting point, affinity-triggered heparin/VEGF hydrogels have shown the ability to respond to the presence of VEGF receptors with consequent hydrogel degradation [73].

Manipulating more efficiently degradation and the temporal properties of the hydrogel network is another important issue to consider in the future development of affinity-triggered hydrogels [130]. The spatiotemporal control over the material's properties can be performed over a range of cell- and tissue-relevant length scales, with no toxic by-products. This can be particularly interesting for cell encapsulation, where a uniform distribution of cells is desired [129]. This is a feature that has not yet been explored for affinity-triggered hydrogels and could benefit both tissue engineering and drug release applications.

Over the last 20 years, a great progress has been made in the exploitation of known affinity pairs ligand-receptor to assemble hydrogels for biomedical applications. Such a large body of knowledge serve as the basis to understand the systems from the molecular to the macroscopic levels, and as a consequence to design materials with controlled properties. The possibility to apply design rules in such affinity-triggered hydrogels will likely expand the solutions offered to other fields of knowledge than biomedicine, namely interfacing electronics and devices.

Acknowledgements

The authors acknowledge funding from the Applied Molecular Biosciences Unit - UCIBIO (UIDB/04378/2020), PTDC/BII-BIO/28878/2017, and the research fellowship SFRH/BPD/97585/2013 for A.S.P., and PD/BD/105871/2014 for C.S.M.F., which are financed by national funds from Fundação para a Ciência e Tecnologia.

References

[1] A.M.G.C. Dias, O. Iranzo, A.C.A. Roque, Affinity adsorbents for proline-rich peptide sequences: a new role for WW domains, RSC Adv. 6 (2016) 68979–6. doi:10.1039/C6RA10900D.

[2] I.L. Batalha, H. Zhou, K. Lilley, C.R. Lowe, A.C.A. Roque, Mimicking nature: Phosphopeptide enrichment using combinatorial libraries of affinity ligands, J. Chromatogr. A. 1457 (2016) 76–87. doi:10.1016/j.chroma.2016.06.032.

[3] A. Pina, S. Carvalho, A. Margarida, G.C. Dias, M. Guilherme, A.S. Pereira, L.T. Caraca, A. Sofia, C.R. Lowe, A. Roque, Tryptophan tags and de novo designed complementary affinity ligands for the expression and purification of recombinant proteins, J. Chromatogr. A. 1472 (2016) 55–65. doi:10.1016/j.chroma.2016.10.017.

[4] R. dos Santos, A.L. Carvalho, A.C.A. Roque, Renaissance of protein crystallization and precipitation in biopharmaceuticals purification, Biotechnol. Adv. 35 (2017) 41–50.

[5] A.M.G.C. Dias, A. Roque, The future of protein scaffolds as affinity reagents for purification, Biotechnol. Bioeng. 114 (2017) 481–491.

[6] J. Garousi, S. Lindbo, B. Mitran, J. Buijs, V. Anzhelika, V. Tolmachev, S. Hober, Comparative evaluation of tumor targeting using the anti-HER2 ADAPT scaffold protein labeled at the C-terminus with indium-111 or technetium-99m, Sci. Rep. 7 (2017) 1–11. doi:10.1038/s41598-017-15366-w.

[7] S. Ståhl, T. Gräslund, A. Eriksson, F.Y. Frejd, P.-åke Nygren, J. Löfblom, Affibody Molecules in Biotechnological and Medical Applications, Trends Biotechnol. 35 (2017) 691–712. doi:10.1016/j.tibtech.2017.04.007.

[8] X. Dou, T. Nomoto, H. Takemoto, M. Matsui, K. Tomoda, Effect of multiple cyclic RGD peptides on tumor accumulation and intratumoral distribution of IRDye 700DX-conjugated polymers, Sci. Rep. 8 (2018) 1–12. doi:10.1038/s41598-018-26593-0.

[9] C.T.S. Wong, P. Foo, J. Seok, W. Mulyasasmita, A. Parisi-amon, S.C. Heilshorn, Two-component protein-engineered physical hydrogels for cell encapsulation, Proc. Natl. Acad. Sci. 106 (2009) 22067–22072.

[10] M.S. Thompson, M. V Tsurkan, K. Chwalek, M. Bornhauser, M. Schlierf, C. Werner, Y. Zhang, Self-assembling hydrogels crosslinked solely by receptor-ligand interactions: Tunability, rationalization of physical properties, and 3D cell culture, Chem. - A Eur. J. 21 (2015) 3178–3182. doi:10.1002/chem.201406366.

[11] F. Ito, K. Usui, D. Kawahara, A. Suenaga, T. Maki, S. Kidoaki, H. Suzuki, M. Taiji, M. Itoh, Y. Hayashizaki, T. Matsuda, Reversible hydrogel formation driven by protein-peptide-specific interaction and chondrocyte entrapment, Biomaterials. 31 (2010) 58–66. doi:10.1016/j.biomaterials.2009.09.026.

[12] L. Zou, C.J. Addonizio, B. Su, M.J. Sis, A.S. Braegelman, D. Liu, M.J. Webber, Supramolecular Hydrogels via Light-Responsive Homoternary cross-links, Biomacromolecules. (2020) 10.1021/acs.biomac.0c00950. doi:10.1021/acs.biomac.0c00950.

[13] Q. Feng, J. Xu, K. Zhang, H. Yao, N. Zheng, L. Zheng, J. Wang, K. Wei, X. Xiao, L. Qin, L.

Bian, Dynamic and Cell-Infiltratable Hydrogels as Injectable Carrier of Therapeutic Cells and Drugs for Treating Challenging Bone Defects, ACS Cent. Sci. 5 (2019) 440–450. doi:10.1021/acscentsci.8b00764.
[14] Q. Feng, K. Wei, S. Lin, Z. Xu, Y. Sun, P. Shi, G. Li, L. Bian, Mechanically resilient , injectable , and bioadhesive supramolecular gelatin hydrogels crosslinked by weak host-guest interactions assist cell in filtration and in situ tissue regeneration, Biomaterials. 101 (2016) 217–228. doi:10.1016/j.biomaterials.2016.05.043.
[15] K. Zhang, Z. Jia, B. Yang, Q. Feng, X. Xu, W. Yuan, X. Li, X. Chen, L. Duan, D. Wang, L. Bian, Adaptable Hydrogels Mediate Cofactor-Assisted Activation of Biomarker-Responsive Drug Delivery via Positive Feedback for Enhanced Tissue Regeneration, Adv. Sci. 5 (2018). doi:10.1002/advs.201800875.
[16] S.C. Grindy, R. Learsch, D. Mozhdehi, J. Cheng, D.G. Barrett, Z. Guan, P.B. Messersmith, N. Holten-andersen, Control of hierarchical polymer mechanics with bioinspired metal-coordination dynamics, Nat. Mater. (2015) 1–8. doi:10.1038/NMAT4401.
[17] M.J. Rowland, C.C. Parkins, J.H. Mcabee, A.K. Kolb, R. Hein, X.J. Loh, C. Watts, O.A. Scherman, An adherent tissue-inspired hydrogel delivery vehicle utilised in primary human glioma models, Biomaterials. 179 (2018) 199. doi:10.1016/j.biomaterials.2018.05.054.
[18] M. Guvendiren, H.D. Lu, J. a. Burdick, Shear-thinning hydrogels for biomedical applications, Soft Matter. 8 (2012) 260. doi:10.1039/c1sm06513k.
[19] R.A. Marklein, J.A. Burdick, Controlling stem cell fate with material design, Adv. Mater. 22 (2010) 175–189. doi:10.1002/adma.200901055.
[20] A.M. Jonker, D.W.P.M. Löwik, J.C.M. Van Hest, Peptide- and protein-based hydrogels, Chem. Mater. 24 (2012) 759–773. doi:10.1021/cm202640w.
[21] F. Edalat, H. Bae, S. Manoucheri, J.M. Cha, A. Khademhosseini, Engineering Approaches Toward Deconstructing and Controlling the Stem Cell Environment, Annu. Biomed. Eng. 40 (2012) 1301–1315. doi:10.1007/s10439-011-0452-9.Engineering.
[22] O. Wichterle, D. Lím, Hydrophilic Gels for Biological Use, Nature. 185 (1960) 117–118.
[23] D.T. Chang, R. Chai, R. Dimarco, S.C. Heilshorn, A.G. Cheng, Protein-engineered hydrogel encapsulation for 3-D culture of murine cochlea, Otol. Neurotol. 36 (2014) 531–538.
[24] L. Cai, R.E. Dewi, S.C. Heilshorn, Injectable hydrogels with in situ double network formation enhance retention of transplanted stem cells, Adv. Funct. Mater. 25 (2015) 1344–1351. doi:10.1002/adfm.201403631.
[25] A. Parisi-Amon, W. Mulyasasmita, C. Chung, S.C. Heilshorn, Protein-engineered injectable hydrogel to improve retention of transplanted adipose-derived stem cells, Adv. Healthc. Mater. 2 (2013) 428–432. doi:10.1002/adhm.201200293.
[26] T. Takei, H. Nakahara, K. Kawakami, Synthesis of a chitosan derivative soluble at neutral pH and gellable by freeze–thawing, and its application in wound care, Acta Biomater. 8 (2012) 686–693.
[27] R.N. Shah, N.A. Shah, M.M. Del Rosario Lim, C. Hsieh, G. Nuber, S.I. Stupp, Supramolecular design of self-assembling nanofibers for cartilage regeneration., Proc. Natl. Acad. Sci. U. S. A. 107 (2010) 3293–3298. doi:10.1073/pnas.0906501107.
[28] C. Chung, B.L. Pruitt, S.C. Heilshorn, Spontaneous cardiomyocyte differentiation of mouse embryoid bodies regulated by hydrogel crosslink density, Biomater. Sci. 1 (2013) 1082–1090. doi:10.1039/C3BM60139K.
[29] Y.P. Lu, C.H. Yang, J.A. Yeh, F.H. Ho, Y.C. Ou, C.H. Chen, M.Y. Lin, K.S. Huang, Guidance of neural regeneration on the biomimetic nanostructured matrix, Int. J. Pharm. 463 (2014) 177–183. doi:10.1016/j.ijpharm.2013.08.006.
[30] Y.S. Zhang, A. Khademhosseini, Advances in engineering hydrogels, Science (80-.). 356 (2017) 1–10. doi:10.1126/science.aaf3627.
[31] K. Varaprasad, G. Malegowd, T. Jayaramudu, M. Mohan, R. Sadiku, A mini review on

hydrogels classification and recent developments in miscellaneous applications, Mater. Sci. Eng. C. 79 (2017) 958–971. doi:10.1016/j.msec.2017.05.096.
[32] B.O. Okesola, A. Mata, Multicomponent self-assembly as a tool to harness new properties from peptides and proteins in material design, Chem. Soc. Rev. 47 (2018) 3721–3736. doi:10.1039/C8CS00121A.
[33] O. Boutureira, J.L. Bernardes, Advances in Chemical Protein Modification, Chem. Rev. 115 (2015) 2174–2195. doi:10.1021/cr500399p.
[34] J. Sahoo, C. Pappas, I. Sasselli, Y. Abul-Haija, R. Ulijn, Biocatalytic Self-Assembly Cascades, Angew. Chem. Int. Ed. Engl. 56 (2017) 6828–6832.
[35] M. Ebara, Y. Kotsuchibashi, R. Narain, N. Idota, Y.-J. Kim, J.M. Hoffman, K. Uto, T. Aoyagi, Smart Hydrogels, in: Smart Biomater., 2014: pp. 9–65. doi:10.1007/978-4-431-54400-5.
[36] N. Zanna, A. Merlettini, G. Tatulli, L. Milli, M.L. Focarete, C. Tomasini, Hydrogelation Induced by Fmoc-Protected Peptidomimetics, Langmuir. 31 (2015) 12240–12250.
[37] S. Kundu, Y. M, S. M, Effect of salt content on the rheological properties of hydrogel based on oligomeric electrolyte, J. Phys. Chem. B. 114 (2010) 1541–1457.
[38] J. Raeburn, C. Mendoza-Cuenca, B.N. Cattoz, M.A. Little, A.E. Terry, A.Z. Cardoso, P.C. Griffiths, D.J. Adams, The effect of solvent choice on the gelation and final hydrogel properties of Fmoc–diphenylalanine, Soft Matter. 11 (2015) 927–935.
[39] I.P. Moreira, T.K. Piskorz, J.H. van Esch, T. Tuttle, R. V Ulijn, Biocatalytic Self-Assembly of Tripeptide Gels and Emulsions, Langmuir. 33 (2017) 4986–4995.
[40] J.R. McDaniel, I. Weitzhandler, S. Prevost, K.B. Vargo, M.-S. Appavou, D.A. Hammer, M. Gradzielski, A. Chilkoti, Noncanonical Self-Assembly of Highly Asymmetric Genetically Encoded Polypeptide Amphiphiles into Cylindrical Micelles, Nano Lett. 14 (2014) 6590–6598.
[41] Y. Liu, B. Liu, J. Riesberg, W. Shen, In situ forming physical hydrogels for three-dimensional tissue morphogenesis, Macromol. Biosci. 11 (2011) 1325–1330.
[42] C. Sinthuvanich, L.A. Haines-Butterick, K.J. Nagy, J.P. Schneider, Iterative design of peptide-based hydrogels and the effect of network electrostatics on primary chondrocyte behavior, Biomaterials. 33 (2013) 7478–7488.
[43] P. Dankers, T. Hermans, T. Baughman, Y. Kamikawa, R. Kieltyka, M. Bastings, H. Janssen, N. Sommerdijk, A. Larsen, M. van Luyn, A. Bosman, E. Popa, G. Fytas, E. Meijer, Hierarchical formation of supramolecular transient networks in water: a modular injectable delivery system, Adv. Mater. 24 (2012) 2703–2709.
[44] J. Cui, A. del Campo, Multivalent H-bonds for self-healing hydrogels, Chem. Commun. 48 (2012) 9302–9304.
[45] M. Guo, L. Pitet, H. Wyss, M. Vos, P. Dankers, E. Meijer, Tough stimuli-responsive supramolecular hydrogels with hydrogen-bonding network junctions, J. Am. Chem. Soc. 136 (2014) 6969–6977.
[46] V. Gauba, J.D. Hartgerink, Self-Assembled Heterotrimeric Collagen Triple Helices Directed through Electrostatic Interactions, J. Am. Chem. Soc. 129 (2007) 2683–2690.
[47] N.H. Romano, D. Sengupta, C. Chung, S.C. Heilshorn, Protein-engineered biomaterials: nanoscale mimics of the extracellular matrix., Biochim. Biophys. Acta. 1810 (2011) 339–49. doi:10.1016/j.bbagen.2010.07.005.
[48] J.L. Mann, A.C. Yu, G. Agmon, E. Appel, Supramolecular Polymeric Biomaterials, Biomater. Sci. (2017) 10–37. doi:10.1039/C7BM00780A.
[49] S. Harding, B. Chowdhry, Protein-Ligand Interactions : Hydrodynamics and Calorimetry (Practical Approach Series), Oxford University Press, 2001.
[50] R.J.F. Branco, A.M.G.C. Dias, A. Roque, Understanding the molecular recognition between antibody fragments and protein A biomimetic ligand., J. Chromatogr. A. 1244 (2012) 106–

15. doi:10.1016/j.chroma.2012.04.071.
[51] N. Yamaguchi, K.L. Kiick, Polysaccharide-poly(ethylene glycol) star copolymer as a scaffold for the production of bioactive hydrogels, Biomacromolecules. 6 (2005) 1921–1930. doi:10.1021/bm050003+.
[52] H.K. Lau, K.L. Kiick, Opportunities for Multicomponent Hybrid Hydrogels in Biomedical Applications, Biomacromolecules. 16 (2014) 28–42.
[53] D. Sengupta, S.C. Heilshorn, Protein-engineered biomaterials: highly tunable tissue engineering scaffolds, Tissue Eng. Part B. Rev. 16 (2010) 285–293. doi:10.1089/ten.teb.2009.0591.
[54] R.L. Dimarco, S.C. Heilshorn, Multifunctional materials through modular protein engineering, Adv. Mater. 24 (2012) 3923–3940. doi:10.1002/adma.201200051.
[55] K. Saha, A.J. Keung, E.F. Irwin, Y. Li, L. Little, D. V. Schaffer, K.E. Healy, Substrate modulus directs neural stem cell behavior, Biophys. J. 95 (2008) 4426–4438. doi:10.1529/biophysj.108.132217.
[56] L. Cai, C.B. Dinh, S.C. Heilshorn, One-pot synthesis of elastin-like polypeptide hydrogels with grafted VEGF-mimetic peptides, Biomater. Sci. 2 (2014) 757. doi:10.1039/C3BM60293A.
[57] W.Y. Seow, C. a. E. Hauser, Short to ultrashort peptide hydrogels for biomedical uses, Mater. Today. 17 (2014) 381–388. doi:10.1016/j.mattod.2014.04.028.
[58] X. Jia, K.L. Kiick, Hybrid multicomponent hydrogels for tissue engineering, Macromol. Biosci. 9 (2009) 140–156. doi:10.1002/mabi.200800284.
[59] E. Dawson, G. Mapili, K. Erickson, S. Taqvi, K. Roy, Biomaterials for stem cell differentiation, Adv. Drug Deliv. Rev. 60 (2008) 215–228. doi:10.1016/j.addr.2007.08.037.
[60] J. Kopeček, J. Yang, Smart Self-Assembled Hybrid Hydrogel Biomaterials, Angew. Chem. Int. Ed. Engl. 51 (2012) 7396–7417. doi:10.1126/science.1249098.Sleep.
[61] M. Kumar, N.L. Ing, V. Narang, N.K. Wijerathne, A.I. Hochbaum, R. Ulijn, Amino-acid-encoded biocatalytic self-assembly enables the formation of transient conducting nanostructures, Nat. Chem. 10 (2018) 696–703. doi:10.1038/s41557-018-0047-2.
[62] N. Annabi, Y. Zhang, A. Assmann, E.S. Sani, G. Cheng, A.D. Lassaletta, A. Vegh, B. Dehghani, G.U. Ruiz-esparza, X. Wang, S. Gangadharan, A. Weiss, A. Khademhosseini, Engineering a highly elastic human protein – based sealant for surgical applications, Sci. Transl. Med. 9 (2017) 1–14.
[63] J. Li, D.J. Mooney, Designing hydrogels for controlled drug delivery, Nat. Rev. Mater. 1 (2016) 1–18. doi:10.1038/natrevmats.2016.71.
[64] V. Huynh, R.G. Wylie, Competitive Affinity Release for Long-Term Delivery of Antibodies from Hydrogels, Angew. Chemie - Int. Ed. 57 (2018) 3406–3410. doi:10.1002/anie.201713428.
[65] M. Cianchetti, C. Laschi, A. Menciassi, P. Dario, Biomedical applications of soft robotics, Nat. Rev. Mater. xx (2018) xx. doi:10.1038/s41578-018-0022-y.
[66] S. Yoon, J.K. Sim, Y.-H. Cho, C. Liu, C. Xu, A Flexible and Wearable Human Stress Monitoring Patch, Sci. Rep. 6 (2016) 23468. doi:10.1038/srep23468.
[67] A. Hussain, A.T.S. Semeano, S.I.C.J. Palma, A.S. Pina, J. Almeida, B.F. Medrado, A.C.C.S. Pádua, A.L. Carvalho, M. Dionísio, R.W.C. Li, H. Gamboa, R. V. Ulijn, J. Gruber, A.C.A. Roque, Tunable gas sensing gels by cooperative assembly, Adv. Funct. Mater. 27 (2017) 1700803. doi:DOI: 10.1002/adfm.201700803.
[68] L.D. Eramo, B. Chollet, M. Leman, E. Martwong, M. Li, H. Geisler, J. Dupire, M. Kerdraon, C. Vergne, F. Monti, Y. Tran, P. Tabeling, Microfluidic actuators based on temperature-responsive hydrogels, Nat. Publ. Gr. 4 (2018) 1–7. doi:10.1038/micronano.2017.69.
[69] T.B.H. Schroeder, A. Guha, A. Lamoureux, G. Vanrenterghem, D. Sept, M. Shtein, J. Yang, M. Mayer, An electric-eel-inspired soft power source from stacked hydrogels, Nature. 552

(2017) 214–218. doi:10.1038/nature24670.
[70] C.A. Custódio, R.L. Reis, J.F. Mano, Engineering Biomolecular Microenvironments for Cell Instructive Biomaterials, Adv. Healthc. Mater. 3 (2014) 797–810. doi:10.1002/adhm.201300603.
[71] K. Szaciłowski, W. Macyk, A. Drzewiecka-Matuszek, M. Brindell, G. Stochel, Bioinorganic photochemistry: Frontiers and mechanisms, Chem. Rev. 105 (2005) 2647–2694. doi:10.1021/cr030707e.
[72] J. Thiele, Y. Ma, S.M.C. Bruekers, S. Ma, W.T.S. Huck, Designer hydrogels for cell cultures: A materials selection guide, Adv. Mater. 26 (2014) 125–148. doi:10.1002/adma.201302958.
[73] N. Yamaguchi, L. Zhang, B.S. Chae, C.S. Palla, E.M. Furst, K.L. Kiick, Growth factor mediated assembly of cell-receptor-responsive hydrogels, J. Am. Chem. Soc. 129 (2007) 3040–3041. doi:10.1021/ja0680358.
[74] L. Zhang, E.M. Furst, K.L. Kiick, Manipulation of hydrogel assembly and growth factor delivery via the use of peptide-polysaccharide interactions, J. Control. Release. 114 (2006) 130–142. doi:10.1016/j.jconrel.2006.06.005.
[75] T. Miyata, T. Uragami, K. Nakamae, Biomolecule-sensitive hydrogels, Adv. Drug Deliv. Rev. 54 (2002) 79–98. doi:10.1016/S0169-409X(01)00241-1.
[76] R.D. Gray, R.H. Glew, The Kinetics of Carbohydrate Binding to Concanavalin A, J. Biol. Chem. 248 (1973) 7547–7551.
[77] A.A. Obaidat, K. Park, Characterization of glucose dependent gel-sol phase transition of the polymeric glucose-concanavalin a hydrogel system, Pharm. Res. 13 (1996) 989–995. doi:10.1023/A:1016090103979.
[78] A.A. Obaidat, K. Park, Characterization of protein release through glucose-sensitive hydrogel membranes, Biomaterials. 18 (1997) 801–806. doi:10.1016/S0142-9612(96)00198-6.
[79] S.J. Lee, K. Park, Synthesis and characterization of sol-gel phase-reversible hydrogels sensitive to glucose., J. Mol. Recognit. 9 (1996) 549–557. doi:10.1002/(SICI)1099-1352(199634/12)9:5/6<549::AID-JMR299>3.0.CO;2-C.
[80] T. Miyata, A. Jikihara, K. Nakamae, Preparation of poly (2-glucosyloxyethyl methacrylate) - concanavalin A complex hydrogel and its glucose-sensitivity, Macromol. Chem. Phys. 1146 (1996) 1135–1146.
[81] T. Miyata, N. Asami, T. Uragami, A reversibly antigen-responsive hydrogel., Nature. 399 (1999) 766–769. doi:10.1038/21619.
[82] T. Miyata, N. Asami, T. Uragami, Structural Design of Stimuli-Responsive Bioconjugated Hydrogels That Respond to a Target Antigen, J. Polym. Sci. Part B Polym. Phys. 47 (2009) 2144–2157. doi:10.1002/polb.
[83] R.J. Gübeli, D. Hövermann, H. Seitz, B. Rebmann, R.G. Schoenmakers, M. Ehrbar, G. Charpin-El Hamri, M. Daoud-El Baba, M. Werner, M. Müller, W. Weber, Remote-controlled hydrogel depots for time-scheduled vaccination, Adv. Funct. Mater. 23 (2013) 5355–5362. doi:10.1002/adfm.201300875.
[84] Y. Liu, J. Liu, J. Xu, S. Feng, T.P. Davis, Biodegradable PEG hydrogels cross-linked using biotin-avidin interactions, Aust. J. Chem. 63 (2010) 1413–1417. doi:10.1071/CH10168.
[85] J. Clapper, M. Pearce, C.A. Guymon, A. Salem, Biotinylated biodegradable nanotemplated hydrogel networks for cell interactive applications, Biomacrmolecules. 9 (2008) 1188–1194.
[86] R.Y. Tam, M.J. Cooke, M.S. Schoichet, A covalently modified hydrogel blend of hyaluronan–methyl cellulose with peptides and growth factors influences neural stem/progenitor cell fate, Jounral Mater. Chem. 22 (2012) 19402–19411.
[87] R. Wylie, S. Ahsan, Y. Aizawa, K. Maxwell, C. Morshead, M. Shoichet, Spatially controlled simultaneous patterning of multiple growth factors in three-dimensional hydrogels., Nat.

Mater. 10 (2011) 799–806.
[88] R. Barbucci, A. Magnani, C. Roncolini, S. Silvestri, Antigen–antibody recognition by Fourier transform IR spectroscopy/attenuated total reflection studies: Biotin–avidin complex as an example, Biopolymers. 31 (1991) 827–834. doi:10.1002/bip.360310703.
[89] J. DeChancie, K. Houk, The Origins of Femtomolar Protein - Ligand Binding : Hydrogen-Bond Cooperativity and Desolvation Energetics in the Biotin - (Strept) Avidin Binding Site, J. Am. Chem. Soc. 129 (2007) 5419–5429. doi:10.1021/ja066950n.
[90] Y. Cui, Y. Li, Q. Duan, T. Kakuchi, Preparation of hyaluronic acid micro-hydrogel by biotin-avidin-specific bonding for doxorubicin-targeted delivery, Appl. Biochem. Biotechnol. 169 (2013) 239–249. doi:10.1007/s12010-012-9968-1.
[91] C.S. Fernandes, A.L. Rodrigues, V.D. Alves, s T.D. Fernande, A.S. Pina, A.C.A. Roque, Natural multimerization rules the performance of affinity-based physical hydrogels for stem cell encapsulation and differentiation, Biomacromolecules. (2020). doi:10.1021/acs.biomac.0c00473.
[92] D.E. Hoke, D.D. Carson, M. Höök, A heparin binding synthetic peptide from human HIP / RPL29 fails to specifically differentiate between anticoagulantly active and inactive species of heparin, J. Negat. Results Biomed. 2 (2003).
[93] S. Ashikari-Hada, H. Habuchi, Y. Kariya, K. Kimata, Heparin Regulates Vascular Endothelial Growth Factor165-dependent Mitogenic Activity, Tube Formation, and Its Receptor Phosphorylation of Human Endothelial Cells, J. F Biol. Chem. 280 (2005) 31508–31515.
[94] T.Z. Grove, C.O. Osuji, J.D. Forster, E.R. Dufresne, L. Regan, Stimuli-responsive smart gels realized via modular protein design, J. Am. Chem. Soc. 132 (2010) 14024–14026. doi:10.1021/ja106619w.
[95] B.L. Seal, A. Panitch, Physical polymer matrices based on affinity interactions between peptides and polysaccharides., Biomacromolecules. 4 (2003) 1572–1582. doi:10.1021/bm0342032.
[96] B.L. Seal, A. Panitch, Viscoelastic behavior of environmentally sensitive biomimetic polymer matrices, Macromolelcules. 39 (2006) 2268–2274. doi:10.1021/ma0524528.
[97] S. Mohanty, M. Ovee, M. Banerjee, PDZ Domain Recognition: Insight from Human Tax-Interacting Protein 1 (TIP-1) Interaction with Target Proteins, Biol. 4 (2015) 88–103.
[98] X. Yan, H. Zhou, J. Zhang, C. Shi, X. Xie, Y. Wu, C. Tian, Y. Shen, J. Long, Molecular Mechanism of Inward Rectifier Potassium Channel 2.3 Regulation by Tax-Interacting Protein-1, J. Mol. Biol. 392 (2009) 967–976.
[99] D. Guan, M. Ramirez, L. Shao, D. Jacobsen, I. Barrera, J. Lutkenhaus, Z. Chen, Two-component protein hydrogels assembled using an engineered disulfide-forming protein-ligand pair., Biomacromolecules. 14 (2013) 2909–16. doi:10.1021/bm400814u.
[100] J. Wang, J. Zhang, X. Zhang, H. Zhou, A protein-based hydrogel for in vitro expansion of mesenchymal stem cells., PLoS One. 8 (2013) e75727. doi:10.1371/journal.pone.0075727.
[101] X. Zhang, X. Chu, L. Wang, H. Wang, G. Liang, J. Zhang, J. Long, Z. Yang, Rational design of a tetrameric protein to enhance interactions between self-assembled fibers gives molecular hydrogels, Angew. Chemie - Int. Ed. 51 (2012) 4388–4392. doi:10.1002/anie.201108612.
[102] X. Zhang, H. Zhou, Y. Xie, C. Ren, D. Ding, J. Long, Z. Yang, Rational Design of Multifunctional Hetero-Hexameric Proteins for Hydrogel Formation and Controlled Delivery of Bioactive Molecules., Adv. Healthc. Mater. (2014) 1–8. doi:10.1002/adhm.201300660.
[103] H.D. Lu, M.B. Charati, I.L. Kim, J.A. Burdick, Injectable shear-thinning hydrogels engineered with a self-assembling dock-and-lock mechanism, Biomaterials. 33 (2012) 2145–2153. doi:10.1016/j.biomaterials.2011.11.076.
[104] M.G. Gold, B. Lygren, P. Dokurno, N. Hoshi, G. McConnachie, K. LTaskén, C.R. Carlson, J.D. Scott, D. Barford, Molecular Basis of AKAP Specificity for PKA Regulatory Subunits,

Mol. Cell. 24 (2006) 383–395.
[105] H.D. Lu, D.E. Soranno, C.B. Rodell, I.L. Kim, J.A. Burdick, Secondary photocrosslinking of injectable shear-thinning dock-and-lock hydrogels, Adv. Healthc. Mater. 2 (2013) 1028–1036. doi:10.1002/adhm.201200343.
[106] C. Chang, E. Rossi, D. Goldenberg, The dock and lock method: a novel platform technology for building multivalent, multifunctional structures of defined composition with retained bioactivity, Clin. Cancer Res. 13 (2007) 5586–5591.
[107] S. Topp, V. Prasad, G.C. Cianci, E.R. Weeks, J.P. Gallivan, A genetic toolbox for creating reversible Ca2+-sensitive materials, J. Am. Chem. Soc. 128 (2006) 13994–13995. doi:10.1021/ja064546i.
[108] M. Aoyagi, A.S. Arvai, J.A. Tainer, E.D. Getzoff, Structural basis for endothelial nitric oxide synthase binding to calmodulin, EMBO J. 4 (22AD).
[109] K.L. Yap, T. Yuan, T.K. Mal, H.J. Vogel, M. Ikura, Structural Basis for Simultaneous Binding of Two Carboxy-terminal Peptides of Plant Glutamate Decarboxylase to Calmodulin, J. Mol. Biol. 328 (2003) 193–204.
[110] M. Sudol, H.I. Chen, C. Bougeret, A. Einbond, P. Bork, Characterization of a novel protein-binding module--the WW domain., FEBS Lett. 369 (1995) 67–71. doi:10.1016/0014-5793(95)00550-S.
[111] M. Sudol, T. Hunter, NeW wrinkles for an old domain, Cell. 103 (2000) 1001–1004. doi:10.1016/S0092-8674(00)00203-8.
[112] W. Mulyasasmita, L. Cai, Y. Hori, S.C. Heilshorn, Avidity-controlled delivery of angiogenic peptides from injectable molecular-recognition hydrogels, Tissue Eng. Part A. 19 (2014) 1–13. doi:10.1089/ten.tea.2013.0357.
[113] W. Mulyasasmita, L. Cai, R.E. Dewi, A. Jha, S.D. Ullmann, R.H. Luong, N.F. Huang, S.C. Heilshorn, Avidity-controlled hydrogels for injectable co-delivery of induced pluripotent stem cell-derived endothelial cells and growth factors, J. Control. Release. 191 (2014) 71–81. doi:10.1016/j.jconrel.2014.05.015.
[114] W. Mulyasasmita, J.S. Lee, S.C. Heilshorn, Molecular-level engineering of protein physical hydrogels for predictive sol-gel phase behavior., Biomacromolecules. 12 (2011) 3406–11. doi:10.1021/bm200959e.
[115] C.S. Fernandes, A.J. Barbosa, F. Duarte, V. Alves, P. Gomes, T. Fernandes, A.S. Pina, A.C.A. Roque, An affinity-triggered hydrogel based on a designed peptide-peptide affinity pair, Biomacromolecules. (2020).
[116] C. Scheufler, A. Brinker, G. Bourenkov, S. Pegoraro, L. Moroder, H. Bartunik, F.U. Hartl, I. Moarefi, Structure of TPR Domain–Peptide Complexes: Critical Elements in the Assembly of the Hsp70–Hsp90 Multichaperone Machine, Cell. 101 (2000) 199–210.
[117] T.Z. Grove, J. Forster, G. Pimienta, E. Dufresne, L. Regan, A modular approach to the design of protein-based smart gels, Biopolymers. 97 (2012) 508–517. doi:10.1002/bip.22033.
[118] M. Ehrbar, R. Schoenmakers, E.H. Christen, M. Fussenegger, W. Weber, Drug-sensing hydrogels for the inducible release of biopharmaceuticals, Nat. Mater. 7 (2008) 800–804. doi:10.1038/nmat2250.
[119] I.M. Martins, R.L. Reis, H.S. Azevedo, Phage display technology in biomaterials engineering: Progress and opportunities for applications in regenerative medicine, ACS Chem. Biol. 11 (2016) 2962–2980. doi:10.1021/acschembio.5b00717.
[120] J. Wu, P. Li, C. Dong, H. Jiang, B. Xue, X. Gao, M. Qin, W. Wang, B. Chen, Y. Cao, Rationally designed synthetic protein hydrogels with predictable mechanical properties, Nat. Commun. 9 (2018) 1–11. doi:10.1038/s41467-018-02917-6.
[121] S. Huang, J. Shen, N. Li, M. Ye, Dual pH- and Temperature-Responsive Hydrogels with Extraordinary Swelling / Deswelling Behavior and Enhanced Mechanical Performances, J. Appl. Polym. Sci. 41530 (2015) 1–9. doi:10.1002/app.41530.

[122] M.J. Webber, Engineering responsive supramolecular biomaterials: Toward smart therapeutics, Bioeng. Transl. Med. 1 (2016) 252–266. doi:10.1002/btm2.10031.
[123] M.C. Koetting, J.T. Peters, S.D. Steichen, N.A. Peppas, Stimulus-responsive hydrogels: Theory, modern advances, and applications, Mater. Sci. Eng. R. 93 (2015) 1–49. doi:10.1016/j.mser.2015.04.001.
[124] A.M. Kloxin, A.M. Kasko, C.N. Salinas, K.S. Anseth, Photodegradable hydrogels for dynamic tuning of physical and chemical properties, Science (80-.). 324 (2009) 59–63. doi:10.1126/science.1169494.Photodegradable.
[125] S. Yagai, A. Kitamura, Recent advances in photoresponsive supramolecular self-assemblies, in: Chem. Soc. Rev., 2008: pp. 1520–1529. doi:10.1039/b703092b.
[126] W. Petka, J. Harden, K. McGrath, D. Wirtz, D. Tirrell, Reversible hydrogels from self-assembling artificial proteins, Science (80-.). 28 (1998) 389–392.
[127] O. Pieroni, A. Fissi, N. Angelini, F. Lenci, Photoresponsive polypeptides, Acc. Chem. Res. 34 (2001) 9–17. doi:10.1021/ar990141+.
[128] M.E. Byrne, K. Park, N.A. Peppas, Molecular imprinting within hydrogels, Adv. Drug Deliv. Rev. 54 (2002) 149–161. doi:10.1016/S0169-409X(01)00246-0.
[129] J.A. Burdick, W.L. Murphy, Moving from static to dynamic complexity in hydrogel design, Nat. Commun. 3 (2012) 1–8. doi:10.1038/ncomms2271.
[130] T.E. Brown, K.S. Anseth, Spatiotemporal hydrogel biomaterials for regenerative medicine, Chem. Soc. Rev. 46 (2017) 6532–6552.
[131] C.S. Fernandes, A.L. Rodrigues, V.D. Alves, T.G. Fernandes, A.S. Pina, A.C.A. Roque, Natural multimerization rules the performance of affinity-based physical hydrogels for stem cell encapsulation and differentiation, Biomacrmolecules. Just accep (2020). doi:10.1021/acs.biomac.0c00473.

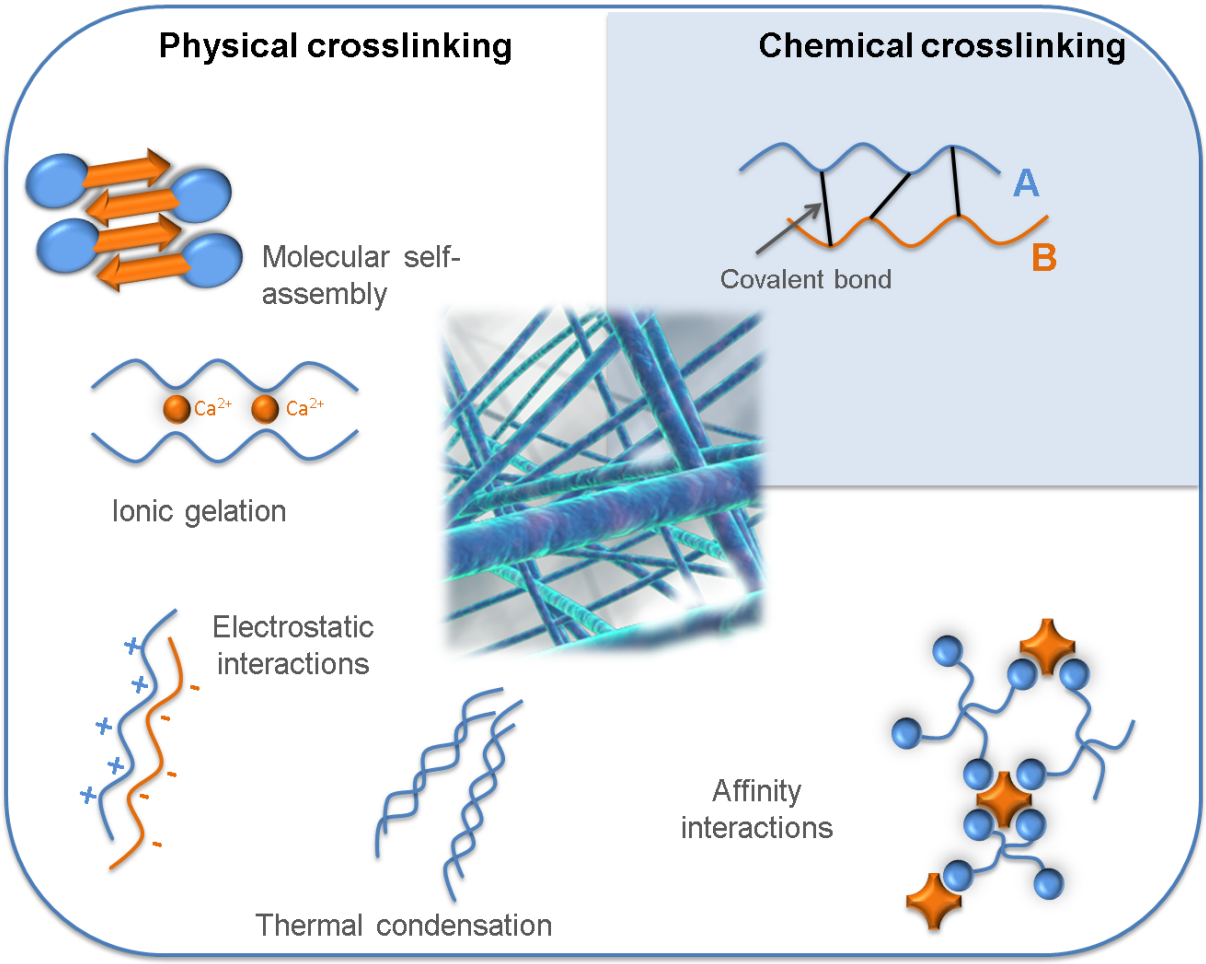

Figure 1. Classification of hydrogels according to the crosslinking mechanism used during production. Chemical cross-linked hydrogels assemble due to the establishment of covalent bonds between compatible reactive ends in polymeric chains A and B (A and B can be the same or different). Covalent bonds are formed due to a chemical reaction triggered by chemical crosslinkers, light or catalysts. Physical cross-linked hydrogels assemble due to the establishment of specific non-covalent interactions (affinity interactions) or due to the establishment of non-specific non-covalent interactions, namely electrostatic interactions and π-π interactions.

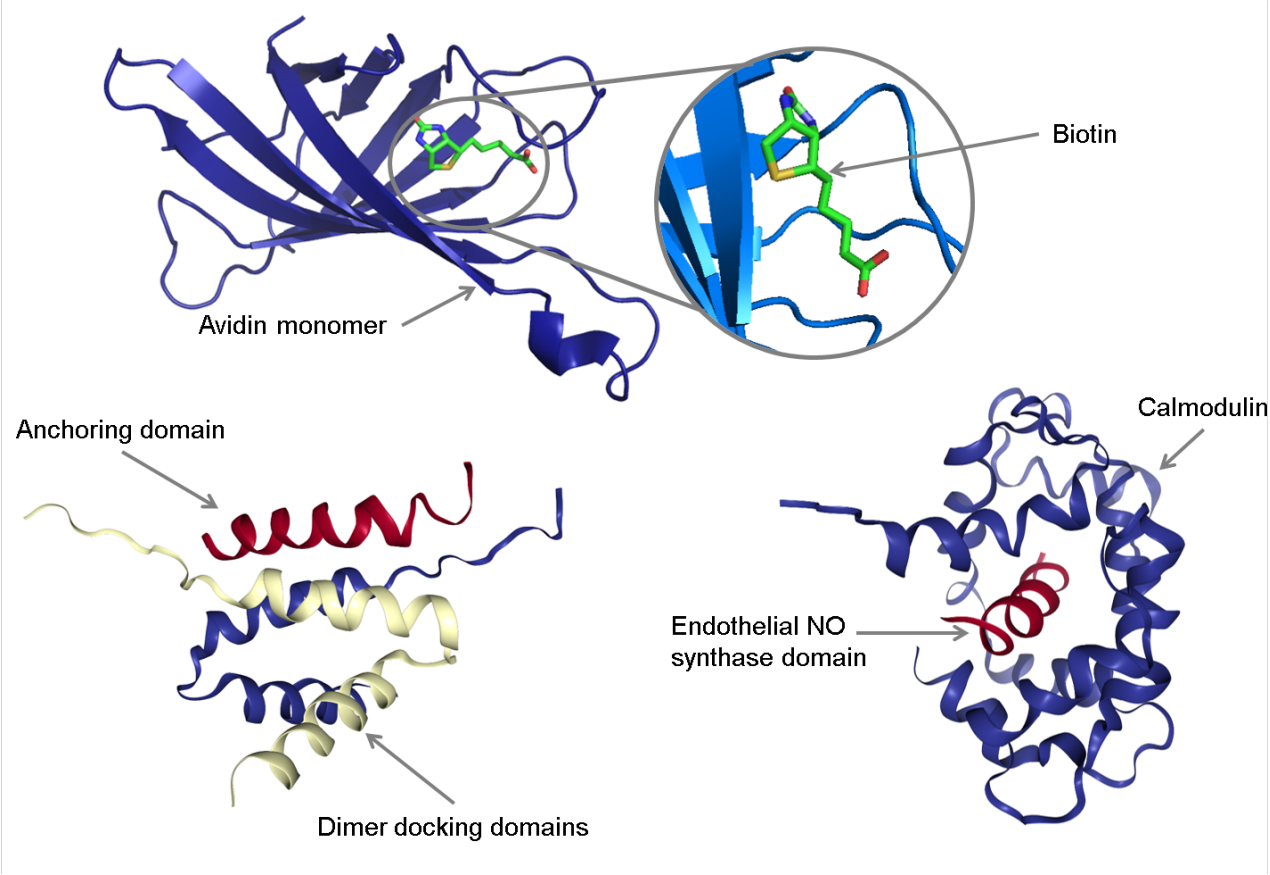

Figure 2. Examples of ligand-receptor affinity pairs used to generate affinity-triggered hydrogels.

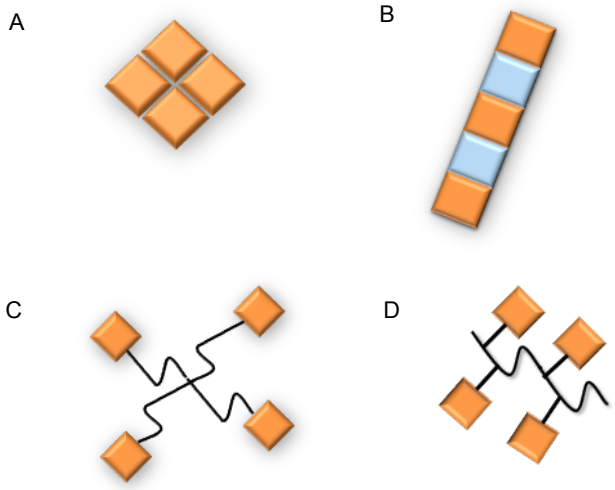

Figure 3. Schematic representation of the typical ways to generate multivalent display of affinity pair components, as (A) multimeric proteins, (B) in tandem separated by a spacer (in blue), or attached to a (C) star branched or (D) linear branched polymer.

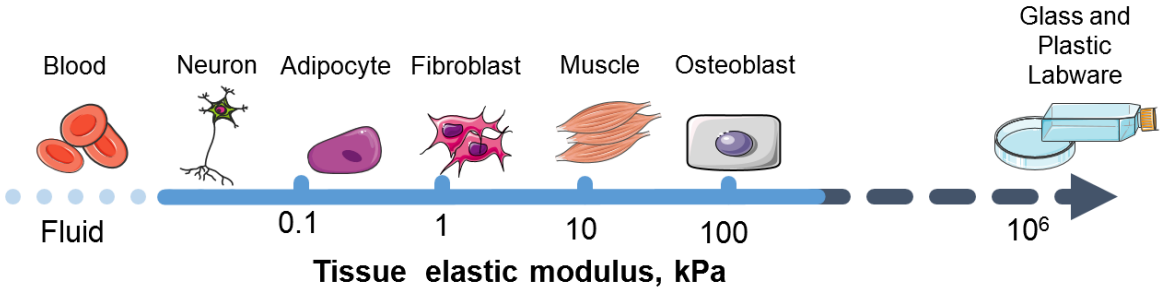

Figure 4- In the body, solid tissues display different stiffness, as measured by the elastic modulus in kPa.

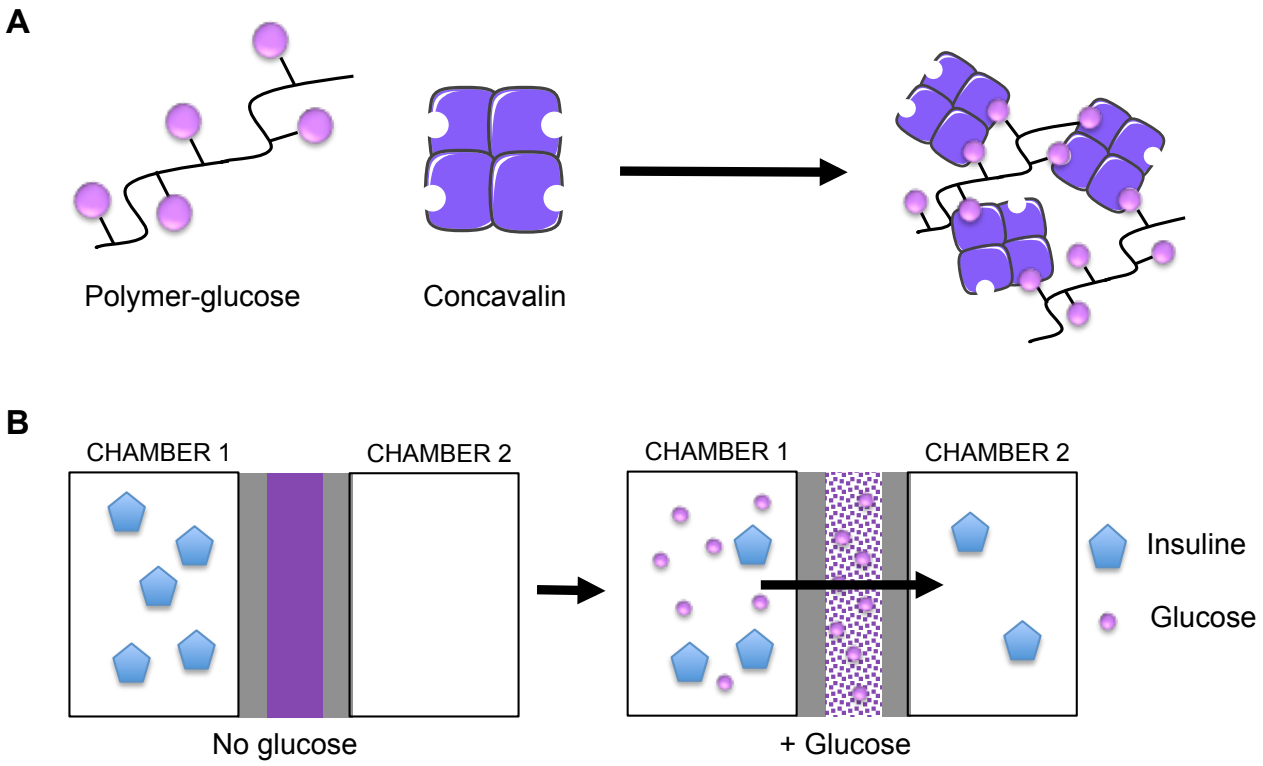

Figure 5 – (A) Schematic representation of an affinity-triggered hydrogel self-assembly based on the affinity pair glucose and concanavalin [77–79]. (B) Using the affinity-triggered hydrogel as a self-regulating insulin delivery system.

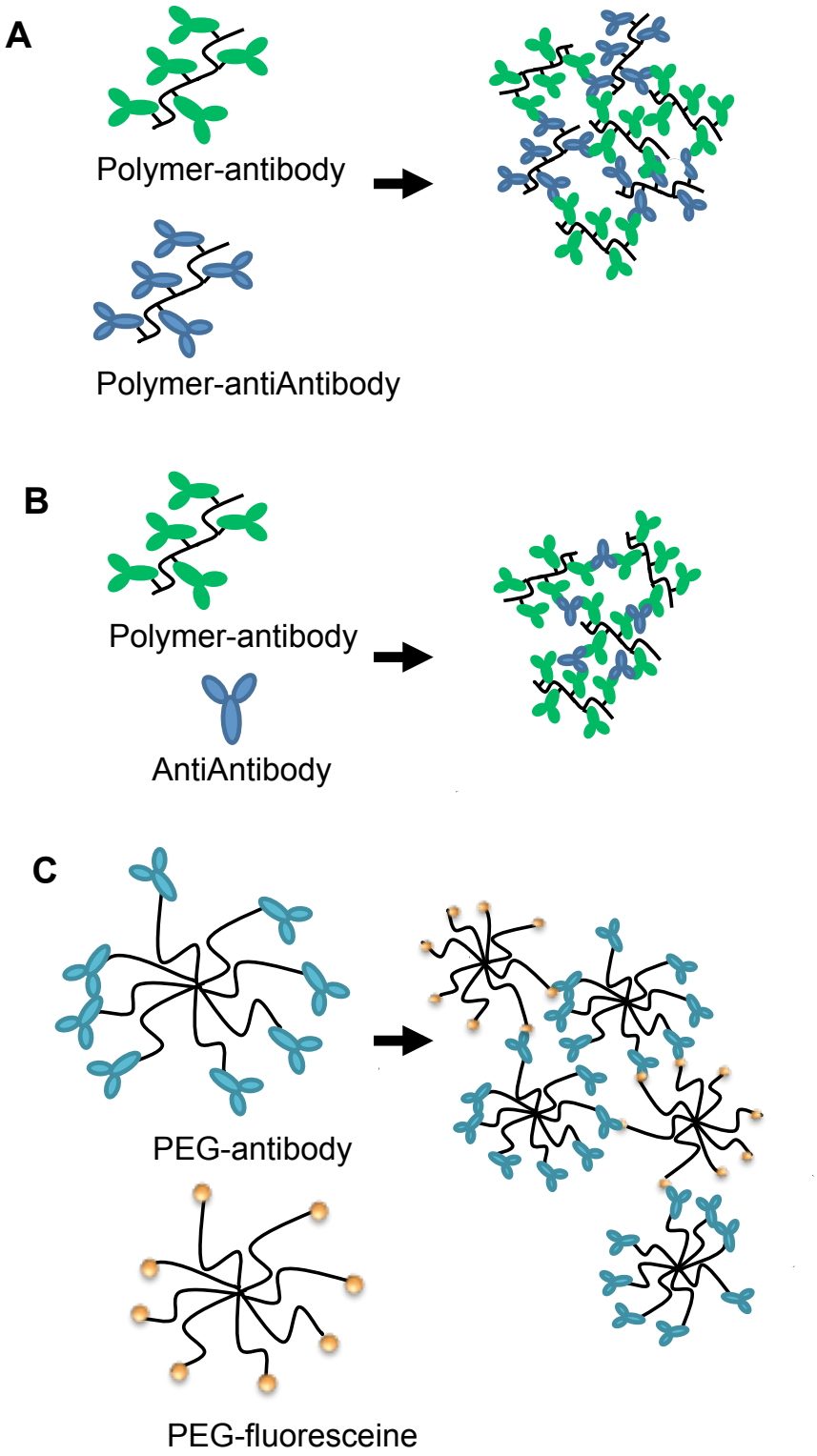

Figure 6 - (A) Schematic representation of an affinity-triggered hydrogel self-assembly based on the affinity pair antibody/antigen, where the antigen is an anti-antibody molecule (semi-interpenetrating polymer network) [81]. (B) Schematic representation of an affinity-triggered hydrogel self-assembly based on the affinity pair antibody/antigen (antibody-antigen entrapment hydrogels) [82]. (C) Schematic representation of an affinity-triggered hydrogel self-assembly based on the affinity pair antibody/fluorescein [83].

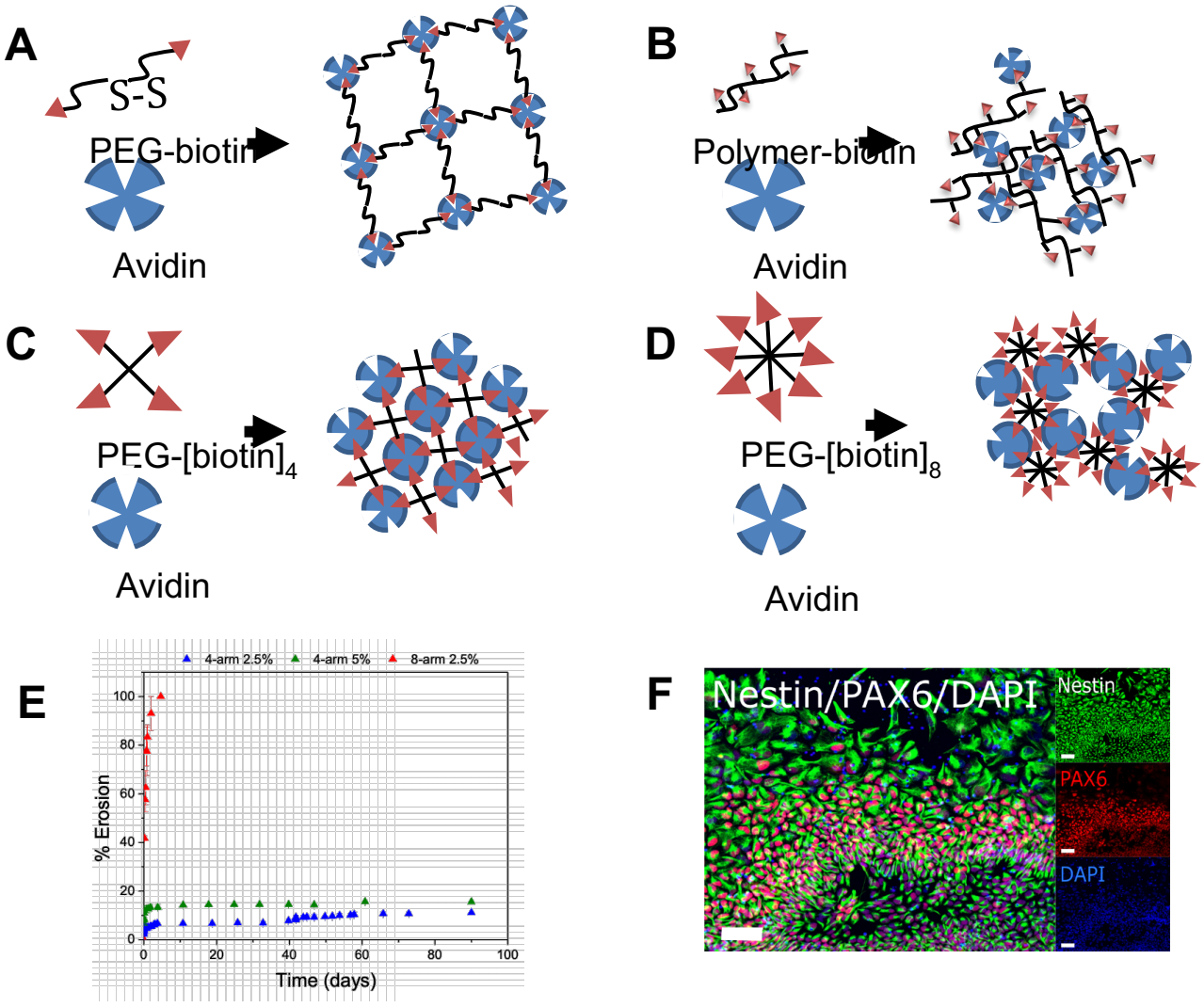

Figure 7 - (A) Schematic representation of an affinity-triggered hydrogel based on the affinity pair biotin and avidin [84]. (B) Schematic representation of an affinity-triggered hydrogel self-assembly based on the affinity pair biotin (immobilized on hyaluronic acid) and avidin [90]. (C) Schematic representation of an affinity-triggered hydrogel based on the affinity pair biotin (conjugated to 4-arm PEG) and avidin [131]. (D) Schematic representation of an affinity-triggered hydrogel based on the affinity pair biotin (conjugated to 8-arm PEG) and avidin [131]. (E) Erosion profile or avidin/PEG-biotin hydrogels [131]. (F) Immunocytochemistry of replated aggregates after encapsulation for neural differentiation markers: Nestin (green) co-marked with PAX6 (red). DAPI was used to counterstain nuclei [131].

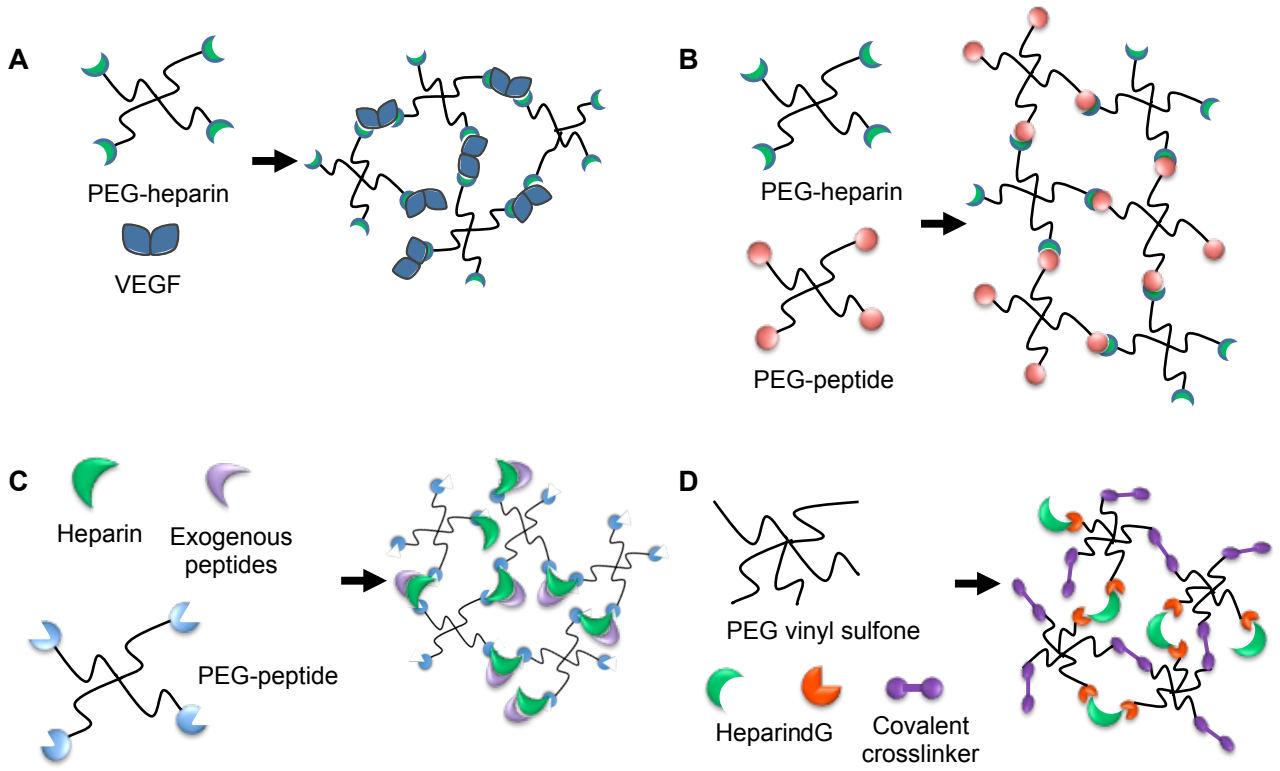

Figure 8 – (A) Schematic representation of an affinity-triggered hydrogel self-assembly based on the affinity pair vascular endothelial growth factor (VEGF) and low molecular weight heparin [73]. (B) Schematic representation of an affinity-triggered hydrogel self-assembly based on the affinity pair and low molecular weight heparin (LMWH) and heparin binding peptides - HIP peptide (CRPKAKAKAKAKDQTK) [51] and $PF4_{ZIP}$ (CGGRMKQLEDKVKKLLKKNYHLENEVARLKKLVG) [74]. (C) Schematic representation of an affinity-triggered hydrogel self-assembly based on the affinity pair heparin and heparin-binding peptides for the capture of exogenous heparin binding peptides [95]. (D) Schematic of a hydrogel incorporating covalent and physical crosslinks (dG, dansyl- GKAFAKLAARLYRKAGC; covalent crosslinker, GCRGDSGPQGIAGQGC) [96].

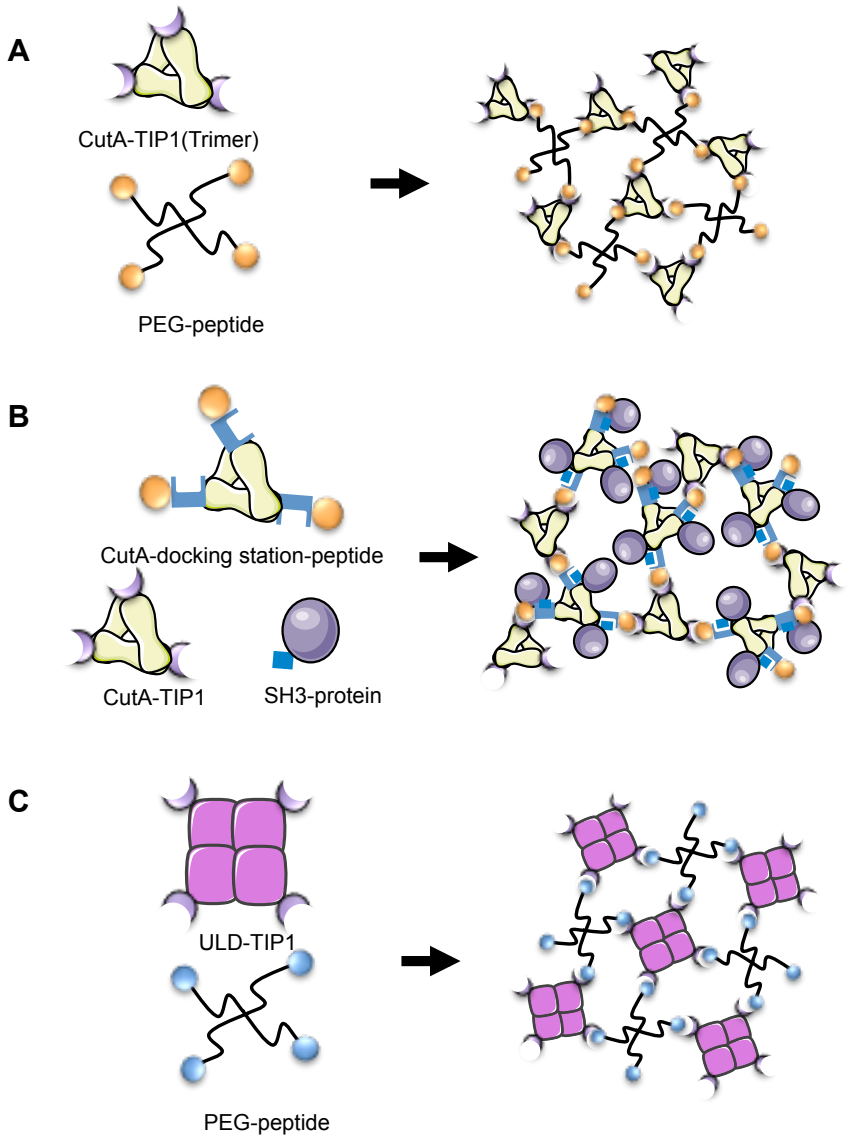

Figure 9 – (A) Schematic representation of an affinity-triggered hydrogel self-assembly based on the affinity pair TIP1 (fused to CutA) and a TIP1-binding peptide [11]. (B) Schematic representation of an affinity-triggered hydrogel self-assembly based on the affinity pair TIP1 (fused to CutA) and a TIP1-binding peptide (fused to CutA and a docking station peptide) [99]. (C) Schematic representation of an affinity-triggered hydrogel self-assembly based on the affinity pair TIP1 (fused to ubiquitin-like domain) and a TIP1-binding peptide [100].

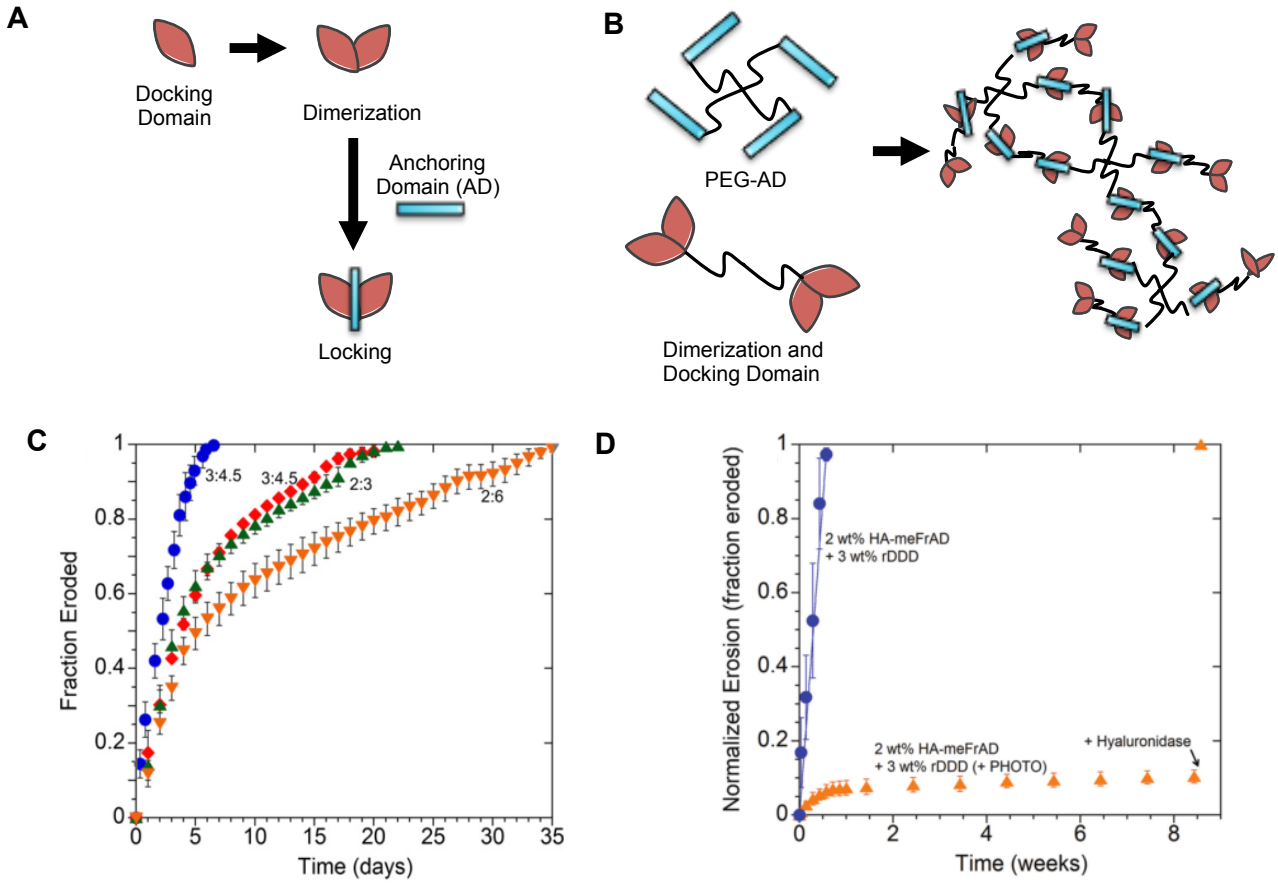

Figure 10- (A) Schematic representation of the Docking and Dimerization Domain and Anchoring Domain and (B) their interaction to form an affinity-triggered hydrogel self-assembly, based on physical crosslinks [103]. (C) Fraction eroded over time for hydrogels composed by ratios of the Docking and Dimerization Domain and Anchoring Domain. [103] Reprinted from Injectable shear-thinning hydrogels engineered with a self-assembling Dock-and-Lock mechanism, 33, H. D. Lu, M. B. Charati, I. L. Kim, J. A. Burdick, 2145, Copyright (2012), with permission from Elsevier. (D) Fraction eroded over time for physical (blue) and physical and chemical (orange) hydrogels. The addition of hyaluronidase resulted in instant hydrogel erosion [103]. Reprinted from Injectable shear-thinning hydrogels engineered with a self-assembling Dock-and-Lock mechanism, 33, H. D. Lu, M. B. Charati, I. L. Kim, J. A. Burdick, 2145, Copyright (2012), with permission from Elsevier.

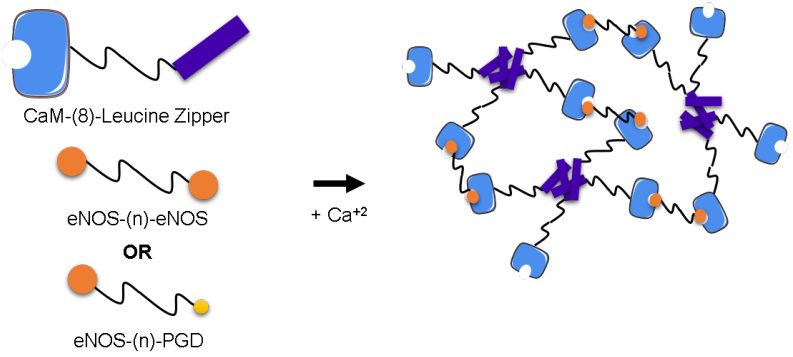

Figure 11 – Schematic representation of an affinity-triggered hydrogel self-assembly based on the affinity pair CaM and calmodulin-binding domains (eNOS and PGD) [107].

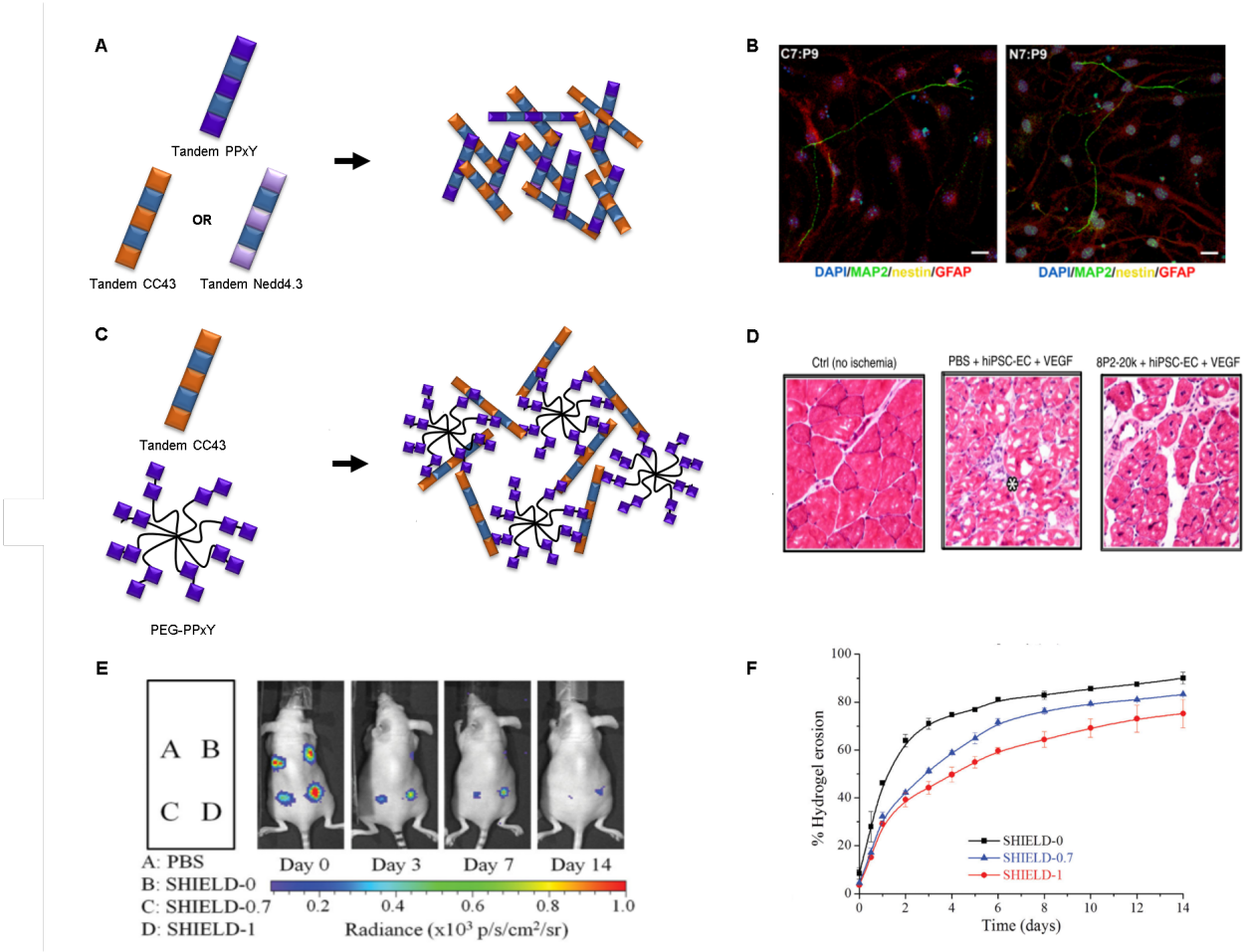

Figure 12 - (A) Schematic representation of affinity-triggered hydrogels based on the affinity pair WWin blue domain (CC43 in orange or Nedd4.3 in yellow, separated by a spacer in blue) and a proline rich peptide using tandem protein display (PPxY in purple, separated by a spacer in blue). The number of repeats varied from 7-9 [9]. (B) Encapsulated adult neural stem cell differentiation at 6 days of culture (red, glial marker GFAP; green, neuronal marker MAP2; yellow, progenitor marker nestin; blue, nuclei, DAPI). Scale bar, 25 μm [9]. Copyright (2013), with permission from Wiley**.** (C) Schematic representation of affinity-triggered hydrogels based on the affinity pair WW domain and a proline rich peptide. The WW domain is displayed in tandem (9 repeats, in orange separated by a spacer in blue) and the proline-rich peptide (in purple) is conjugated to a 8-arm PEG molecule [113]. (D) Photomicrographs of cryo-sectioned samples of skeletal muscles 14 days after femoral artery ligation-induced ischemia (hematoxylin and eosin (H&E) staining). Inflammation of connective tissues is marked with asterisk. Reprinted from Avidity-controlled hydrogels for injectable co-delivery of induced pluripotent stem cell-derived endothelial cells and growth factors, 191, W. Mulyasasmita, L. Cai, R. E. Dewi, A. Jha, S. D. Ullmann, R. H. Luong, N. F. Huang, S. C. Heilshorn, 71, Copyright (2014), with permission from Elsevier**.** (E) Cell retention after *in vivo* subcutaneous injection of encapsulated human adipose-derived stem cells in double physical network hydrogels at 0, 3, 7, and 14 days post-injection [24]. Copyright (2015), with permission from Wiley. (F) Erosion kinetics of double physical crosslinked hydrogels over time [24]. Copyright (2015), with permission from Wiley.

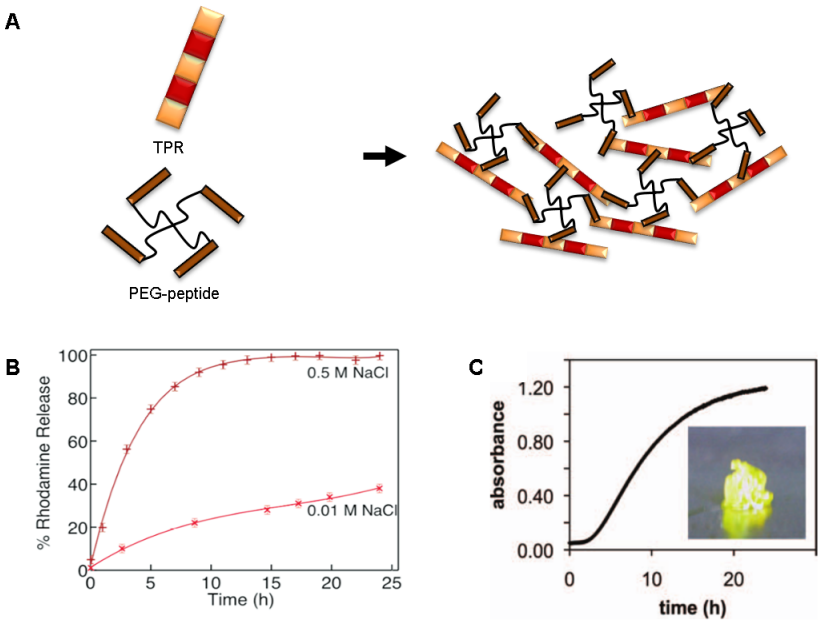

Figure 13 - (A) Schematic representation of an affinity-triggered hydrogel self-assembly based on the affinity between tetratricopeptide repeat (TPR) domains (in light green separated by a spacer in red) and peptide ligands (dark green) [94]. (B) Rhodamine release profile over time from the TRP/peptide ligands affinity-triggered hydrogels at two different ionic strengths. Reprinted with permission from [94]. Copyright 2010 American Chemical Society. (C) Anticancer compound release profile from TRP/peptide ligand affinity-triggered hydrogels [117]. Copyright (2012), with permission from Wiley.

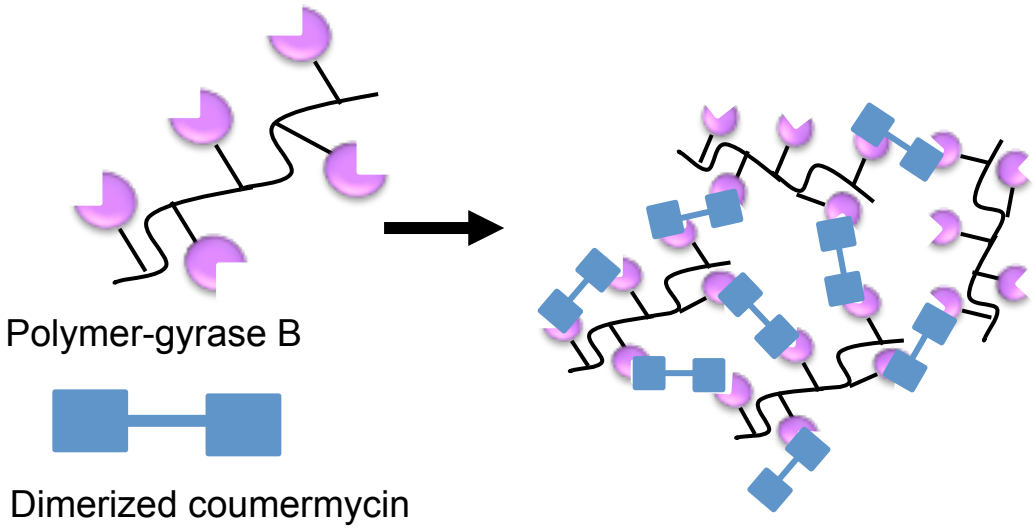

Figure 14 - Schematic representation of an affinity-triggered hydrogel self-assembly based on the affinity between bacterial gyrase subunit B and coumermycin [118].

Table 1. Comparison between physically and chemically cross-linked hydrogels.

Physical	Chemical
Network maintained by physical interactions	Network maintained by covalent bonds
Independent of crosslinkers or organic solvents	May require chemical crosslinkers or catalysts, often toxic
Lower mechanical resistance	Higher mechanical resistance
Rapid erosion	Slower erosion
No significant volume change upon gel transition	Significant volume change upon gel transition
Dynamic crosslinks does not lead to spatial inhomogeneity of the mechanical properties	Erosion leads to spatial inhomogeneity of the mechanical properties
Susceptible to shear-stress	Require hydrolytic or enzyme degradation for cell applications
Degradation usually leads to non-toxic by-products	Degradation may lead to toxic and non-compatible by-products

Table 2. Ligand-receptor pairs employed to generate 2-component affinity-triggered hydrogels. The molecular weight of each component and peptides sequence (one letter code) is summarized, as well as the reported affinity constants for the ligand-receptor complex. (na –not available)

	Component 1	Component 2	Affinity Constant k_A (M^{-1})
Peptide-peptide	WW domain Nedd4 (3.9 kDa)	Proline-rich peptide (1.5 kDa) EYPPYPPPPYPSG	$1.6x10^4$
	WW domain CC43 (4.3 kDa)	Proline-rich peptide (1.5 kDa) EYPPYPPPPYPSG	$2.2x10^5$
	Truncated WW (1.6 kDa)	Proline-rich peptide (1.5 kDa) EYPPYPPPPYPSG	$1.6x10^5$
Protein-peptide	Tax-Interacting protein 1 (14.4 kDa)	β-catenin analogue peptide ligand (1.2 kDa) CQLAWFDTDL	$2.3x10^6$
		Computational peptide (1.4 kDa) CGGGRGDGWRESAI	$1.5x10^8$
	Docking domain (17 kDa)	Anchoring domain (3.1 kDa) ESESLIEEAASRIVDAVIEQVKSESECGGG	$1.0x10^9$
	Calmodulin (17 kDa)	Endothelial NO synthase (2.9 kDa) AGRKKTFKEVANAVKISASLMGAERLI	$3.3x10^8$
		Petunia glutamate decarboxylase (3.3 kDa) AGHKKTDSEVQLEMITAWKKFVEEKKKK	$5.0x10^7$
	Tetratricopeptide repeat (14.4 kDa)	Peptide ligand (1 kDa) CGYGGDESVD	$2.0x10^5$
Protein-small ligand	Concavalin A (112 kDa)	Glucose (180.2 g/mol)	$2.0x10^4$
	Anti-fluorescein IgG (150 kDa)	Fluorescein (332.3 g/mol)	na
	Avidin (16.4 kDa)	Biotin (244.3 g/mol)	$1.0x10^{14}$
	Gyrase (24 kDa)	Coumermycin (1.1 kDa)	$1.0x10^8$
Protein-protein	Rabbit IgG (150 kDa)	Anti-rabbit IgG (150 kDa)	$2.6x10^8$
Carbohydrate-protein/peptide	Heparin (3 kDa)	Vascular endothelial growth factor (40 kDa)	$6.0x10^6$
		Heparin interacting peptide (1.8 kDa) CRPKAKAKAKAKDQTK	$2.5x10^5$
		$PF4_{ZIP}$ peptide (3.9 kDa) CGGRMKQLEDKVKKLLKKNYHLENEVARLKKLVG	$1.0x10^5$
		PBD1 peptide (1.8 kDa) KAFAKLAARLYRKAGC	$3.3x10^7$
		W peptide (2.0 kDa) WKAFAKLAARLYRKAGC	na
		dG peptide (1.8 kDa) Dansyl-GKAFAKLAARLYRKAGC	na

Table 3. Affinity-triggered hydrogels for tissue engineering and drug delivery applications.

Hydrogel Property	**Tissue Engineering**	**Drug Delivery**
High water content	Cell compatibility Efficient fluid and gas transport	Allow encapsulation of solvated molecules
Transient physical crosslinks - Self-thinning - Self-healing	Allow cell encapsulation Allow cell delivery to affected site	Control release rate *In situ* delivery of payload as a controlled release depot
Controllable pore size - Polymer concentration - Protein concentration - Density and distance between crosslinks - Molar ratio between components - Affinity between components - Avidity	Efficient nutrients transport Allow cell migration and expansion	Control release rate
Tunable stiffness - Protein concentration - Molar ratio between components - Affinity between components	Stem cell differentiation	Control release rate by addition of inhibitors or by changing environmental conditions
Easy editing of components by molecular biology	Include adhesion and/or recognition motifs Include degradation motifs	Include body degradation motifs (chemical or enzymatic) Include extra adhesion motifs Link between hydrogel component and drug
Biodegradable	Non-toxic by-products	Non-toxic by-products Control drug release

Table 4. Affinity pairs (and respective multimerization strategy) for the development of affinity-triggered hydrogels, their properties and applications.

Component 1	Component 2	Affinity Constant (M^{-1})	Storage Modulus (G', Pa)	Conc. (wt %)	Self-healing time	Erosion	Tissue Engineering Application	Molecule encapsulated	Amount released	Ref
Concanavalin (tetrameric)	Glucose (conjugated to acrylamide)	2×10^4	N/A	10	N/A	N/A	N/A	Lysozyme Insulin	Dependent on external glucose concentration	[78]
Antibody (conjugated to acrylamide)	Antigen (conjugated to acrylamide)	2.6×10^8	N/A	N/A	N/A	N/A	N/A	N/A	N/A	[81]
Antibody (conjugated to multimeric PEG)	Fluorescein (conjugated to multimeric PEG)	N/A	60.5	3	N/A	100 % after 3 days	Induced the immune response in mice with no significant signs of inflammation or rejection	Capsomeres derived from the viral L1 protein	N/A	[83]
Avidin (tetrameric)	Biotin (conjugated to linear PEG oligomer)	10^{15}	N/A	13	N/A	N/A	N/A	N/A	N/A	[84]
	Biotin (conjugated to hyaluronic acid)		N/A	10	N/A	N/A	N/A	Doxorubicin	60 % after 40 hours 90 % 40 hours after incubation with free biotin	[90]
	Biotin (conjugated to linear PEG oligomer)		N/A	4	N/A	100 % after 5 days	Human mesenchymal stromal cells encapsulation; higher cell survival after 24h (95.4 %)	N/A	N/A	[10]
	Biotin (conjugated to 4-arm PEG oligomer)		1.3	2.5	N/A	15 % after 3 months	Encapsulation and support of neural differentiation into a neural lineage of induced pluripotent stem cells	N/A	N/A	[131]
			8.9	5	N/A	10 % after 3 months	N/A	N/A	N/A	
	Biotin (conjugated to 8-arm PEG oligomer)		0.9	2.5	N/A	100 % after 5 hours	N/A	N/A	N/A	
Heparin (conjugated to PEG)	VEGF (dimeric)	6.0×10^6	10	8	N/A	80 % after 4 days	N/A	VEGF	50 % after 10 days	[73]
Heparin (conjugated to multimeric PEG)	HIP (conjugated to multimeric PEG)	2.5×10^5	200	10	N/A	17 % after 4 days	N/A	Basic fibroblast growth factor	16 % after 4 days	[51]

Heparin (conjugated to multimeric PEG)	$PF4_{ZIP}$ (conjugated to multimeric PEG)	$1.0x10^5$	180	2.5	N/A	50 % after 8 days	N/A	Basic fibroblast growth factor	40 % after 8 days	[74]
Heparin (dimeric)	PBD1 (conjugated to multimeric PEG)	$3.3x10^7$	5000 Pa (4ºC) 480 Pa (45ºC)	10	107 seconds	N/A	N/A	Heparin-binding peptides	100 % after 3 days	[95]
Heparin (dimeric)	Heparin-binding peptide W (conjugated to multimeric PEG)	N/A	1060	10	27 minutes	N/A	N/A	N/A	N/A	[96]
	Heparin-binding peptide dG (conjugated to multimeric PEG)	N/A	2760		7.3 minutes					
TIP1 (fused to trimeric protein)	TIP1-binding peptide CQLAWFDTDL (conjugated to multimeric PEG)	$2.3x10^6$	35	4	N/A	N/A	Chondrocytes encapsulation Higher cell viability after 8 day culture	N/A	N/A	[11]
	TIP1-binding peptide CQLAWFDTDL (fused to trimeric protein)	$2.3x10^6$	262	4	N/A	30 % after 28 days	N/A	20 kDa dextran	100 % after 6 days	[99]
								Pyranine	100 % after 4 days	
								Green fluorescent protein	32 % after 7 days	
								Laccase	9 % after 7 days	
TIP1 (fused to tetrameric protein)	TIP1-binding peptide CQLAWFDTDL (conjugated to multimeric PEG)	$1.5x10^8$	80	1	N/A	N/A	Mesenchymal stem cell encapsulation Higher cell viability after 5 day culture	N/A	N/A	[100]
TIP1 (fused to tetrameric protein)	TIP1-binding peptide WRESAI (fused to self-assembly peptide)	$1.5x10^8$	320	5	N/A	N/A	N/A	N/A	N/A	[101]
TIP1 (fused to hexameric protein)	TIP1-binding peptide WRESAI (fused to self-assembly peptide)	$1.5x10^8$	200	0.1	600 seconds	N/A	N/A	Dye-peptide conjugate	50 % after 12 hours	[102]
			400	0.3					20 % after 12 hours	
DDD (conjugated to multimeric PEG)	AD (conjugated to linear spacer)	$1.0x10^9$	300	3	N/A	N/A	N/A	500 Da dextran	100 % after 20 days	[103]
			1000	3	6 seconds	10 % after 2 weeks	Mesenchymal stem cell encapsulation	N/A	N/A	[105]

							Higher cell viability after 3 day culture			
CaM (conjugated to linear polymer)	CaM-binding domains (conjugated to linear polymer)	$3.3x10^8$ (eNOS) $5.0x10^7$ (PGD)	N/A	[2]	N/A	N/A	N/A	N/A	N/A	[107]
WW domain Nedd4.3 (tandem)	Proline-rich peptide (tandem)	$1.6x10^4$	9	10	30 minutes	N/A	N/A	N/A	N/A	[9]
WW domain CC43 (tandem)	Proline-rich peptide (tandem)	$2.2x10^5$	50	10	5 minutes	N/A	PC-12 cells encapsulation; higher cell viability after 5 day culture HUVECs encapsulation; higher cell viability after 5 day culture Murine adult neural stem cells encapsulation and differentiation; higher cell viability after 5 day culture	N/A	N/A	[9]
	Proline-rich peptide (tandem)	$2.2x10^5$	50	10	5 minutes	N/A	Adipose-derived stem cells encapsulation; higher cell viability after 10 day culture Encapsulated adipose-derived stem cells injection into nude mice; higher cell retention after 14 days	N/A	N/A	[25]
	Proline-rich peptide (tandem)	$2.2x10^5$	50	10	5 minutes	N/A	Scratch wound healing assays with HUVECs; more rapid wound closure; network formation HUVEC spheroids encapsulation within a collagen type I and fibronectin matrix; higher outgrowth after 2 day culture	QK (VEGF-mimetic peptide)	60 % (QK-P1) and 50 % (QK-P2) after 21 days	[112]
	Proline-rich peptide (conjugated to multimeric PEG)	$2.2x10^5$	50	10	5 min	50 % after 7 days	hIPCS-EC encapsulation; increased viability after 4 day culture Encapsulated hIPCS-EC injection into mice with induced hindlimb ischemia; reduced necrosis and improved tissue regeneration	20 kDa dextran QK (VEGF-mimetic peptide)	80-90 % after 7 days 80 % after 14 days	[113]

	Proline-rich peptide (conjugated to multimeric PEG)	$2.2x10^5$	100	10	2 seconds	70-90 % after 14 days	Human adipose-derived stem cells encapsulation and transplant into nude mice; higher cell viability after 14 day culture Encapsulated human adipose-derived stem cells injection into murine model; increased cell retention after 3-week experiment	40 kDa dextran	70-100 % after 21 days	[24]
Truncated WW (conjugated to multimeric PEG)	Proline-rich peptide (conjugated to multimeric PEG)	$1.6x10^5$	40	20%	N/A	N/A	Biocompatible	N/A	N/A	[115]
TRP domains (tandem)	Peptide ligands (conjugated to multimeric PEG)	$2.0x10^5$ (10 mM NaCl)	270	[1]	N/A	0 % (0.01 M NaCl) and 100 % (0.5 M NaCl) after 20 days	N/A	Rhodamine	30 % (0.01 M NaCl) and 100 % (0.5 M salt) after 25 hours	[94]
		$3.0x10^4$ (500 mM NaCl)	N/A	[1]	N/A					
Gyrase (conjugated to acrylamide)	Coumermycin (dimeric)	10^8	248	6	N/A	13 % after 12 hours	Human umbilical vein endothelial cells encapsulation; higher viability after 96 hours.	VEGF	Novobiocin concentration dependent	[118]

N/A – not available

[1] Concentration reported by authors: 2 mM

AD - anchoring domain; CaM – calmudolin; DDD - docking and dimerization domain; eNOS - endothelial NO synthase; HIP – heparin interacting protein; hIPCS-EC - human pluripotent stem cell-derived endothelial cells; HUVECs - human umbilical vein endothelial cells; PEG – poly(ethylene) glycol; PGD - petunia glutamate decarboxylase; TIP1- Tax-interacting protein-1; TPR - tetratricopeptide repeat; VEGF – vascular endothelial growth factor.

Multicomponent hydrogels tuned by molecular recognition and designed multivalency

Cláudia S. M. Fernandes, Ana Sofia Pina, Ana Cecília A. Roque*

Keywords: affinity interactions, physical hydrogels, self-assembly, protein materials, multicomponent hydrogels

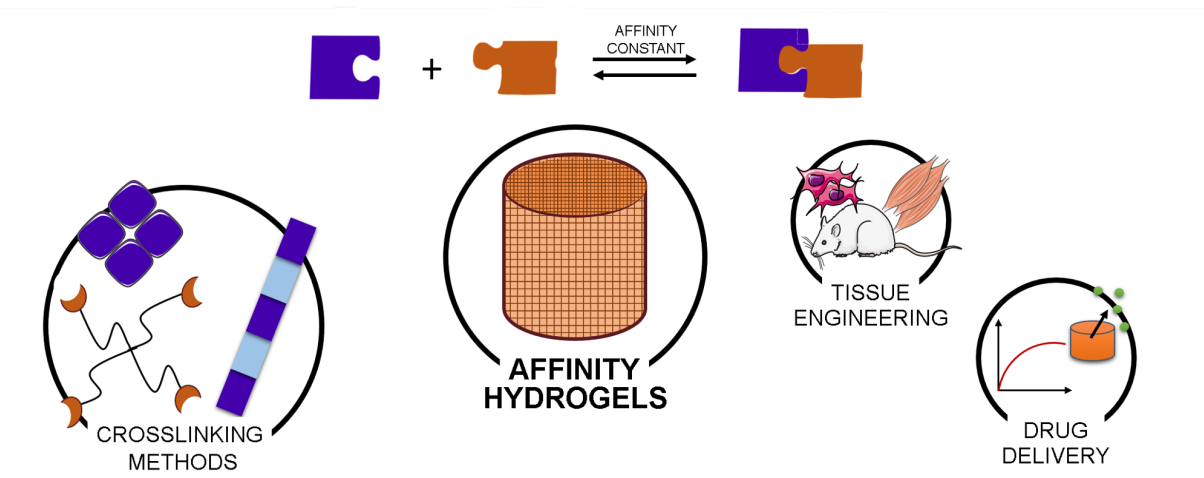

The use of affinity interactions between building blocks comprising ligands and cognate receptors are used as the driving force to trigger the self-assembly process of affinity-triggered hydrogels. This allows the development of novel materials with emergent properties and potential applications in tissue engineering and drug delivery.